Int J Earth Sciences (Geol Rundsch) (2002) 91 : 3–19
DOI 10.1007/s005310100195

ORIGINAL PAPER

A. Gerdes · P. Montero · F. Bea · G. Fershater
N. Borodina · T. Osipova · G. Shardakova

Peraluminous granites frequently with mantle-like isotope compositions: the continental-type Murzinka and Dzhabyk batholiths of the eastern Urals

Received: 2 November 1999 / Accepted: 14 November 2000 / Published online: 7 April 2001

Abstract Murzinka and Dzhabyk are continental-type batholiths of the middle and southern East Uralian domain. They comprise mainly undeformed peraluminous K-rich granites whose elemental composition is similar to some late-Variscan granites of western Europe, but with much more primitive Sr and Nd isotope ratios. Murzinka (254±5 Ma) is composed of silica-rich granites forming two different rock series with a $^{87}Sr/^{86}Sr_{init}$ of 0.709 and 0.704, respectively. Both series have enormous variations in εNd_{255} (–11.9 to –0.1 and –8.9 to +4.1) that reveal derivation from heterogeneous sources. Dzhabyk (291±4 Ma) also comprises two coeval magmas which yielded voluminous granites and quartz-monzonites, respectively, with smaller differences in $^{87}Sr/^{86}Sr_{init}$ and εNd_{290} (~0.7043, +0.8 to +1.6 and ~0.7049, 0.0 to +0.8). Despite their isotope compositions both batholiths lack evidence of genetic involvement of a mantle-derived parental magma. Moreover, we suggest that Dzhabyk granitoids were generated by polybaric partial melting of Paleozoic island-arc material, whereas Murzinka granitoids derived from an extremely heterogeneous source consisting mainly of Paleozoic and Proterozoic metagreywackes. This implies a relative fast reworking of juvenile arc crust and burial of the protoliths during the orogenic evolution of the Urals. Since there is neither evidence of significant extension, nor a direct link with subduction, we suggest that the main cause for late-orogenic anatexis was elevated heat production and fertility in the protolith, perhaps combined with some additional heat from unexposed mafic intrusions.

Keywords Granite genesis · Post-collisional · Ural mountains · Variscan granites · Sr–Nd isotope systematic · Source heterogeneity · Crustal evolution

A. Gerdes (✉) · P. Montero · F. Bea
Department of Mineralogy and Petrology,
University of Granada, Campus Fuentenueva,
18002 Granada, Spain

G. Fershater · N. Borodina · T. Osipova · G. Shardakova
Institute of Geology and Geochemistry,
Russian Academy of Sciences, Pochtovi per. 7,
620219 Ekaterinburg, Russia

Present address:
A. Gerdes
Isotope Geosciences Laboratory, British Geological Survey,
Keyworth Nottingham NG12 5GG, UK
E-mail: ager@bgs.ac.uk
Phone: +44-115-9363260
Fax: 44-115-9363302

Introduction

The middle and southern Urals contain numerous upper-Paleozoic granite batholiths that form several N/S-oriented arrays (Fig. 1; Fershtater et al. 1994). These batholiths display a marked polarity perpendicular to the main axis of the foldbelt, caused by the decreasing age and increasing peraluminosity and concentration of incompatible trace elements to the east (Fershtater et al. 1994, 1998). The western Urals contain abundant lower- to middle-Carboniferous batholiths composed of metaluminous tonalites, trondhjemites, granodiorites and granites intruded into middle-Paleozoic accreted terranes that consist of oceanic and island-arc volcanic rocks (e.g. Bea et al. 1997). The eastern Urals, in contrast, contain upper-Carboniferous to Permian batholiths that comprise mainly peraluminous K-rich granites and granodiorites emplaced in a basement of Proterozoic and Paleozoic gneisses and volcano-sedimentary units (e.g. Fershtater et al. 1994, 1997).

While the early calc-alkaline magmatism of the western Urals seems to be clearly related to the eastward subduction of the Uralian paleo-oceanic crust, the origin and tectonic setting of the dominantly peraluminous granitoids in the continental basement of

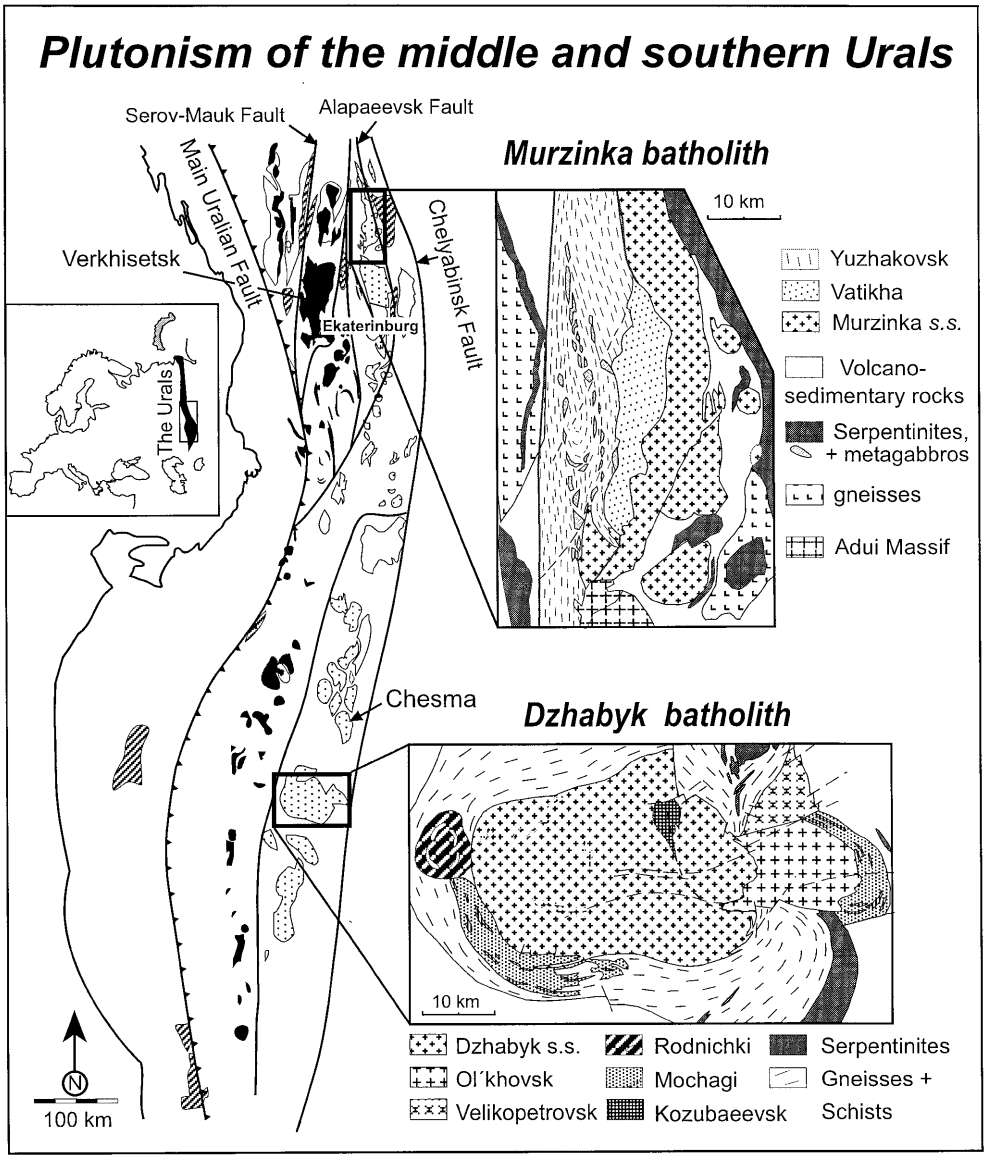

Fig. 1 Geological sketch of the central and southern Urals. Black: subduction-related batholiths. Dotted: continental-type batholiths. Striped: ultramafic massifs. The Murzinka and Dzhabyk batholiths (detailed maps) are representative examples of the continental-type magmatism of the middle and southern Urals

the eastern Urals, hereafter called continental-type granites, still remain obscure.

This paper is a study of the geochemistry, isotope geology and petrogenesis of the continental-type granites of the eastern Urals, which are nearly unknown in the international literature. We summarise herein the results of a field, petrographic, geochemical and Sr–Nd isotope study carried out on the Murzinka and Dzhabyk batholiths from the middle and southern Urals, respectively (Fig. 1). Our aim was to characterise the most important features of late East Uralian magmatism and to give constraints for the possible sources and processes involved in magma genesis.

Geological setting and petrography

The Uralian mobile belt originated during the middle and upper Paleozoic as a consequence of the eastward subduction of the Uralian palaeo-oceanic crust, which was followed by the collision of the eastern European continent with a Siberian-Kazakhian terrane assemblage (e.g. Hamilton 1970; Zonenshain et al. 1990). One of the most outstanding geological features of the Urals is the abundance and variety of middle-Ordovician to Permian magmatic rocks in the region, hereafter named the Uralian domain, which is between the Main Uralian Fault in the west and the Chelyabinsk Fault in the east (Fig. 1). The Uralian Domain consists of a suture sector and two N–S imbricated island-arc continental sectors separated by the Alapaeevsk Fault (Fershtater et al. 1994). The suture sector, representing the palaeo-subduction zone, is a narrow band located immediately east of the Main Uralian Fault. It is characterised by an intense positive gravimetric anomaly and an abundance of mafic-ultramafic complexes that, at least in part, represent fragments of the Uralian palaeo-oceanic crust. The island-arc con-

tinental sectors represent the transition from an oceanic to a continental environment in the middle and southern Urals. They are composed of: (a) an island-arc zone in the west, with abundant basaltic calc-alkaline volcanism; (b) an active continental margin zone in the centre, containing numerous lower- and middle-Carboniferous metaluminous Na-rich granitoids; and (c) a continental zone in the east, characterised by an abundance of upper-Carboniferous to Permian K-rich peraluminous granitoids. Two of the most representative examples for the north and south island-arc continental sectors are the Murzinka and Dzhabyk batholiths (Fershtater et al. 1994). They are composed of similar rocks, mainly peraluminous biotite and two-mica granites, but show important differences in age and isotope composition.

The Murzinka batholith

The Murzinka batholith in the middle Urals is a N/S-elongated granitic complex with maximum dimensions of ~75 km N–S and ~25 km E–W, dated with single-zircon $^{207}Pb/^{206}Pb$ evaporation analyses at 254±5 Ma (Montero et al. 2000). It is west of the Alapaeevsk shear-zone, intruding gneisses, volcano-sedimentary units and serpentinites primarily of Paleozoic age. Barometric data indicate that the equilibration pressure of country rocks decreases from ~0.6 GPa in the west to ~0.4 GPa in the east, due to the post-emplacement eastward tilting of the batholith (Fershtater et al. 1994).

The batholith comprises three units, Yuzhakovsk in the west, Vatikha in the middle and Murzinka s.s. in the east (Fig. 1). Yuzhakovsk granitoids form a network of discordant veins (~0.5–10 m thick) that cut Paleozoic ortho- and paragneisses metamorphosed in the amphibolite facies. Biotite-bearing trondhjemitic and leucogranodioritic veins are distinguished from wider veins with a granitic modal composition. Aplites and pegmatites occur together in both vein types. The K-poor granitoids are characterised by antiperthitic andesine ($An_{30–40}$), red-brown biotite, and apatite and zircon as main accessory phases, whereas the granitic veins have zoned oligoclase ($An_{25–15}$), Ti-rich biotite (TiO_2 ~5%) and magnetite, ilmenite, monazite, sphene and rare almandine garnet as additional accessories. Yuzhakovsk gneisses are intruded by the massive granites of the Vatikha unit, composed of medium-grained, sometimes porphyritic, granites that have aluminous biotite (Al^{IV} ~2.66–2.75 a.f.m.) as the only Fe–Mg mineral. These granites are typified by the presence of conspicuous crystals of oscillatory zoned antiperthitic oligoclase ($An_{24–15}$), highly monoclinic orthoclase, and scarce, but very characteristic, huge crystals of magnetite. The accessory-phases assemblage comprises apatite, zircon, magnetite, ilmenite, monazite, allanite, Th-orthosilicate and xenotime. Medium-grained porphyritic granites of the Murzinka s.s. unit form the main variety of this batholith. These leucocratic granites have abundant veins of aplites and pegmatites, which were the subject of Fersman's classic book on pegmatites (Fersman 1940). The veins can reach a considerable size, up to the point that they are currently mined for gemstones and rare crystals. The mineralogy of Murzinka granites comprises quartz, albitic plagioclase ($An_{18–5}$), porphyritic microcline, aluminous biotite (Al^{IV} ~2.62–2.77 a.f.m.), muscovite and, occasionally, almandine garnet. Magnetite phenocrysts are absent. The accessory mineral assemblage is formed of ilmenite, apatite, zircon, monazite, thorite and xenotime. Murzinka granites show complex intrusive relationships with Vatikha granites, indicating that they were coeval. Both are usually undeformed, except near the eastern contact, where there is a subvertical planar fabric parallel to the Alapaeevsk shear zone (Fig. 1).

The Dzhabyk batholith

The Dzhabyk batholith of the southern Urals is a composite body covering ~65 km W–E and ~35 km N–S (Fig. 1). It is west of the Chelyabinsk fault and intrudes Paleozoic gneisses, schists and serpentinites. It is the only major Uralian batholith with its major axis orientated W–E instead of N–S. Ongoing geophysical research, however, indicates that a considerable part of the batholith is hidden, suggesting it is likely prolonged northwards and connected with the neighbouring Chesma batholith (C. Ayala et al., pers. commun.). The southern part of the Dzhabyk batholith is locally affected by normal shear zones associated with its emplacement. The eastern zone is also affected by a strong regional shear zone.

The Dzhabyk batholith consists of six units: Velikopetrovsk; Ol'khovsk; Dzhabyk s.s.; Rodnichki; Mochagi; and Kozubaeevsk (Fig. 1). Velikopetrovsk is a small body in the NE margin of the batholith. It is composed of deformed medium-grained porphyric biotite granites metamorphosed in the greenschist facies. It probably represents the earliest intrusion. Dzhabyk s.s., which forms the main part of the batholith, is composed of usually porphyritic coarse-, medium- and fine-grained biotite±muscovite granites and leucogranites having sharp intrusive contacts with rocks from the other units. Their modal composition, remarkably constant, is formed of quartz, albite–oligoclase (~$An_{25–10}$), porphyritic K-feldspar, aluminous biotite (Al^{IV}~2.54–2.77 a.f.m.) and, often, primary muscovite, with an accessory mineral assemblage composed of apatite, ilmenite, zircon, monazite and rare xenotime. Ol'khovsk is a concentric intrusion in the east of the batholith, composed of leucocratic, mostly porphyritic, fine- to coarse-grained granites. The main differences with the Dzhabyk s.s. granites are the abundance of grey quartz and microperthitic K-feldspar and an accessory assemblage of titanite, apatite,

frequent magnetite, zircon, allanite and Th-orthosilicate. Dzhabyk s.s. and Ol'khovsk granites have been dated at 291±4 Ma by single-zircon $^{207}Pb/^{206}Pb$ evaporation analysis (Montero et al. 2000).

The Mochagi unit crops out in the eastern and southwestern margins of the batholith (Fig. 1) and was intruded by Dzhabyk granites. This unit and the Rodnichki unit, a concentrically zoned body in the west, comprise quartz-monzonites, quartz-monzodiorites and syenogranites with minor leucogranites. In the case of Rodnichki, they are fine- to medium-grained varieties composed of quartz, K-feldspar, oscillatory-zoned, often antiperthitic, plagioclase (~$An_{35–25}$ to $An_{10–15}$), and moderately aluminous biotite (Al^{IV} ~2.42–2.67 a.f.m.). Mochagi comprises medium- to coarse-grained often porphyric varieties with a well-defined foliation that, apart from biotite, usually contain magnesian hornblende. The accessory assemblage of both units consists of apatite, titanite, titanium-magnetite, zircon, minor allanite, rare thorite and xenotime and monazite in the most felsic varieties.

The small Kozubaeevsk pluton is composed mainly of K-rich mafic to intermediate rocks with a K–Ar amphibole age of ~254±8 Ma (V.I. Kaleganov pers. commun.). It is a late intrusion with a different composition and independent chemical trends (Fershtater et al. 1994) and is considered no further in this article.

Samples and methods

For this work we used the major element data of approximately 240 fresh samples representing all the lithotypes of the Murzinka and Dzhabyk batholiths. A subset of 69 samples was analysed for trace elements (Tables 1 , 2), whereas another subset of 18 samples was also analysed for Sr and Nd isotopes (Table 3). Major element determinations were performed at the IGG (Ekaterinburg) by X-ray fluorescence after fusion with lithium tetraborate. Typical precision was better than ±1.5% for an analyte concentration of 10 wt.%. Trace element determinations were performed under routine conditions at the University of Granada by ICPmass spectrometry (ICP-MS) after HNO_3+HF digestion of 0.100 g of sample powder in a Teflon-lined vessel at ~180 °C and ~200 p.s.i., evaporation to dryness, and subsequent dissolution in 100 ml of 4 vol.% HNO_3. Instrument measurements were carried out in triplicate with a PE SCIEX ELAN-5000 spectrometer using Rh as internal standard and a set of solutions of standard rocks (USGS and CRPG) as external standards. Isobarics were minimised by optimising the plasma torch and numerically corrected by calculating the interference level in each run. Precision, estimated on ten replicates of the standard WS-E (Govindaraju et al. 1994), was better than ±2 and ±5% rel. for analyte concentrations of 50 and 5 ppm, respectively.

Samples for Sr and Nd isotope analyses were digested in the same way using ultra-clean reagents, and analysed at the University of Granada by thermal ionisation mass spectrometry (TIMS) with a Finnigan Mat 262 spectrometer after standard chromatographic separation. Normalisation values were $^{86}Sr/^{88}Sr=0.1194$ and $^{146}Nd/^{144}Nd=0.7219$. Blanks were 0.6 and 0.09 nanograms for Sr and Nd, respectively. Frequent measurements (n=12) of the standard WS-E (Govindaraju et al. 1994) have yielded $^{87}Sr/^{86}Sr=0.706599±11$ (2 s) and $^{143}Nd/^{144}Nd=0.511851±9$ (2 s). $^{87}Rb/^{86}Sr$ and $^{147}Sm/^{144}Nd$ were directly determined by ICP-MS following the method developed by Montero and Bea (1998), with a precision better than 1.2 and 0.9% (2σ), respectively.

Major and trace element geochemistry

The Murzinka batholith

The chemical composition of Murzinka granites is highly variable (Table 1). Yuzhakovsk trondhjemites and leucogranodiorites are K-poor, richer in Ca and Na, but similar in peraluminosity (ASI ~1–1.2) to the granitic veins with $K_2O>Na_2O$ (Fig. 2). Vatikha rocks are peraluminous (ASI ~1.03–1.25) silicic granites with SiO_2 commonly in the range 70–74% and $K_2O>Na_2O$. Murzinka s.s. rocks are high-silica peraluminous (ASI ~1.0–1.22) granites with 72–76% SiO_2 and K_2O~Na_2O. The trace element composition is also extremely variable. Yuzhakovsk rocks are rich in Sr and V, and have variable Nd/Th (~0.7–11) but low Li, Rb, Cs, Be, Ga, Nb, U and Th, with Th/U~7 (Fig. 3). The K-poor granitoids have lower Rb, Ba and Pb contents and more variable K/Rb (283–902, average ~688) in comparison with the granitic veins (K/Rb ~400). Chondrite-normalised REE patterns (see Fig. 5) are commonly characterised by a positive Eu anomaly increasing in intensity with the concentration of Sr (Fig. 4). A positive Ce anomaly is also evident in those samples with elevated Eu anomalies, both anomalies being more intense in the K-poor veins. The LREE/HREE ratios are higher in the granitic than in the K-poor veins (La_N/Yb_N ~78–200 to ~4–70).

Vatikha granites are more uniform than those from Yuzhakovsk. They also have low Li, Be, Cs and U contents; however, their Ba and Sr contents are less high and their Th/U (7–48, average ~18) is more evolved. The Rb, Th, Pb, Nb, Ga and LREE concentrations are variable, although usually higher than in Yuzhakovsk rocks, whereas the K/Rb is lower (230–637, average ~375); however, their range of variation overlaps that of the granitic veins. The Nd/Th ratio is low (0.3–2.7; Fig. 3), usually lower than in common peraluminous crustal rocks with monazite as the major reservoir of Nd and Th (e.g. Bea and Montero 1999). Chondrite-normalised REE patterns range between two extremes (Fig. 5). Samples with low

Table 1 Major (wt %) and trace element (ppm) data of granitoids from the Murzinka batholith. Total Fe as FeO*.

	Yuzhakovsk								Murzinka *s.s.*									Vatikha												
Nr.	**128**	**129**	**114**	**111**	**130**	**76**	**131**	**115**	**22**	**25a**	**26**	**25**	**23**	**50**	**24**	**51**	**42**	**17**	**107**	**95**	**163**	**105**	**106**	**15**	**108**	**66**	**9**	**65**	**10**	**92**	**61**
SiO_2	72.5	72.1	69.8	71.7	71.7	71.4	70.8	70.2	74.2	74.2	74.2	74.1	73.9	73.4	72.8	72.7	72.5	74.7	74.4	73.4	73.2	73.2	73.2	72.9	72.7	72.5	72.0	71.5	71.2	71.1	70.2
TiO_2	0.10	0.14	0.19	0.19	0.13	0.23	0.25	0.26	0.08	0.05	0.10	0.04	0.09	0.09	0.10	0.11	0.14	0.07	0.08	0.05	0.10	0.10	0.17	0.12	0.13	0.14	0.17	0.15	0.24	0.13	0.26
Al_2O_3	15.9	15.8	15.7	14.5	15.5	15.3	15.3	15.1	14.0	14.1	14.2	14.2	13.7	13.9	14.8	14.7	15.3	13.8	13.6	15.1	14.0	14.0	14.3	15.0	13.3	14.9	14.2	15.0	14.7	14.3	14.7
FeO*	1.37	1.69	3.56	2.11	1.57	1.83	1.96	2.28	1.67	1.86	2.35	1.86	2.37	2.62	1.27	1.76	1.67	1.70	2.40	0.87	1.64	2.51	2.32	2.15	3.14	1.66	2.47	1.76	2.98	2.79	3.31
MgO	0.31	0.43	0.61	0.33	0.27	0.50	0.43	0.59	0.11	0.07	0.14	0.07	0.29	0.13	0.14	0.24	0.29	0.11	0.13	0.20	0.21	0.12	0.26	0.24	0.15	0.37	0.33	0.28	0.35	0.31	0.59
MnO	0.00	0.01	0.02	0.01	0.01	0.01	0.01	0.02	0.01	0.01	0.01	0.01	0.02	0.01	0.02	0.01	0.01	0.01	0.01	0.01	0.03	0.01	0.01	0.01	0.02	0.01	0.02	0.01	0.02	0.02	0.02
CaO	2.95	3.00	4.19	1.32	2.11	1.82	1.31	1.46	0.66	0.71	0.80	0.81	1.11	0.74	1.10	1.44	1.48	0.69	0.43	1.06	0.80	0.88	0.93	0.98	0.70	1.40	1.10	1.07	1.19	1.35	1.32
Na_2O	4.82	4.61	3.69	3.94	4.25	3.67	3.94	3.79	3.77	4.22	3.64	4.27	3.51	3.90	4.48	4.50	4.82	3.70	3.87	3.77	3.24	3.96	3.62	3.49	3.26	3.88	3.80	3.39	3.39	3.85	3.67
K_2O	0.81	0.86	0.69	4.84	3.15	4.03	4.61	4.78	4.76	3.66	4.54	3.63	4.50	4.15	4.11	3.34	3.19	4.50	4.08	4.72	5.84	4.52	5.15	4.43	5.29	4.33	3.99	5.39	4.31	4.68	4.65
P_2O_5	0.05	0.05	0.12	0.07	0.11	0.06	0.08	0.09	0.05	0.05	0.05	0.05	0.05	0.05	0.04	0.05	0.05	0.05	0.05	0.01	0.05	0.05	0.05	0.05	0.05	0.05	0.06	0.09	0.07	0.09	0.13
Total	98.8	98.7	98.5	99.0	98.8	98.9	98.6	98.6	99.3	98.9	100.0	99.0	99.5	99.0	98.9	98.8	99.4	99.3	99.0	99.2	99.1	99.3	100.0	99.3	98.7	99.2	98.2	98.6	98.4	98.6	98.9
Li	9	15	13	13	11	13	15	21	17	17	36	22	24	81	23	145	117	17	11	8	11	13	9	13	11	7	18	11	16	11	14
Rb	7	25	14	34	40	77	95	108	220	174	266	236	257	215	240	113	170	164	106	97	148	162	137	124	161	71	105	130	131	95	61
Cs	0.5	0.8	0.4	1.0	0.6	0.4	0.8	1.4	0.9	1.1	2.1	1.2	1.2	6.1	1.2	7.6	5.4	0.7	0.7	0.4	0.6	0.7	0.6	0.6	0.5	0.3	0.8	0.5	0.5	0.3	0.7
Be	1.9	1.5	0.7	1.0	3.5	2.1	1.1	1.5	1.9	3.1	2.6	2.6	2.2	3.3	3.4	5.0	2.5	1.8	1.5	1.7	0.8	1.5	1.3	1.6	0.9	1.8	1.6	1.0	1.4	1.4	1.2
Sr	286	441	533	615	365	869	521	369	72	34	106	61	96	101	44	255	249	96	104	273	272	127	142	89	161	313	126	291	259	292	181
Ba	135	238	78	197	960	1459	1486	1186	292	58	343	112	355	482	132	1185	899	318	312	830	789	427	482	282	749	779	421	850	1055	754	506
Sc	1.3	2.1	10.2	7.5	4.1	4.1	7.5	3.3	2.2	7.2	8.1	3.0	9.6	2.5	3.2	1.9	3.0	2.2	1.7	0.7	6.5	8.2	5.8	6.8	7.7	5.9	2.7	5.6	8.1	5.3	2.9
V	12	18	20	27	9	19	17	18	3.8	1.3	4.7	1.5	2.4	6.2	2.3	12	12	4.1	5.0	2.9	12	5.5	4.1	5.7	5.2	10	14	9	15	10	18
Co	1.3	2.2	2.2	2.4	1.2	4.1	2.5	1.0	0.6	0.2	0.6	0.2	0.6	0.7	0.3	1.5	1.5	0.5	0.1	0.2	1.7	1.4	0.6	0.8	2.0	0.9	0.8	1.8	1.8	1.0	2.3
Zn	11	19	27	53	34	10	33	84	44	30	26	32	38	50	35	81	75	54	30	26	22	13	n.d.	13	36	22	49	11	28	n.d.	57
Ga	17	15	16	16	12	9	9	11	23	25	20	25	21	18	24	19	21	20	18	17	14	18	15	18	14	14	20	14	12	13	20
Y	1.0	3.7	8.0	8.8	5.2	1.0	3.2	3.9	6.5	5.9	6.9	11.7	12.1	4.8	8.3	1.9	2.7	4.7	2.9	1.0	3.6	6.1	9.4	6.8	7.3	2.6	5.6	3.2	6.9	4.2	3.0
Nb	1.3	2.3	4.3	1.3	4.3	2.8	3.3	9.9	14	25	19	17	23	9.7	20	7.0	9.8	9.8	6.8	1.9	16	13	12	11	12	2.8	11	6.9	15	3.4	6.5
Ta	0.1	0.2	1.9	0.1	0.7	0.2	0.3	0.3	0.9	2.4	2.2	1.2	2.4	1.2	2.1	1.4	0.9	0.7	0.3	0.2	3.4	0.8	2.2	1.3	0.5	0.2	0.5	0.4	1.6	0.3	0.3
Zr	54	121	14	13	143	86	213	192	79	39	106	31	103	89	45	78	92	67	93	45	125	107	145	93	183	146	106	75	204	93	130
Hf	1.7	3.2	0.3	0.4	3.0	1.9	3.9	4.9	2.8	1.3	2.8	1.3	2.9	2.9	2.0	2.5	3.1	2.6	3.2	1.4	2.6	2.8	3.5	2.6	4.5	3.1	3.4	1.7	4.4	2.0	3.3
Pb	13	14	7	10	24	18	34	43	39	18	28	39	34	37	38	31	35	43	31	31	23	26	26	25	34	18	30	25	28	21	24
U	0.5	1.9	0.2	0.5	0.6	0.4	1.7	2.0	4.4	2.0	2.9	3.3	5.5	2.3	4.9	1.6	1.9	2.8	1.8	0.4	0.7	2.1	2.6	2.2	2.4	0.7	2.0	0.5	3.1	0.6	0.7
Th	3.5	11	0.5	1.1	6.0	4.2	15	18	19	10	25	12	29	24	14	2.3	4.4	19	17	8	20	34	37	22	35	31	27	4.7	23	26	10
La	3.5	15	5.4	12	13	16	42	27	21	14	45	12	45	21	14	3.7	6.6	22	16	3.8	74	63	76	38	72	14	25	19	63	49	25
Ce	12	39	17	31	45	37	71	54	44	28	84	24	84	44	31	8.5	14	44	36	6.5	146	115	140	73	136	40	61	42	118	89	52
Pr	0.7	3.1	1.5	3.2	3.2	2.8	7.5	5.3	4.5	3.0	9.0	2.5	8.9	4.5	3.2	0.8	1.4	4.6	3.7	0.7	14	12	15	7.9	14	3.0	5.9	4.0	12	9.3	5.9
Nd	2.5	11	6.1	12	12	9	25	18	15	10	29	8	29	15	11	3.0	4.7	16	13	2.3	42	40	49	26	46	11	21	13	37	31	19
Sm	0.6	1.8	1.3	2.0	2.6	1.1	3.4	2.8	3.0	2.4	5.1	2.2	5.9	2.7	2.3	0.6	0.9	3.3	2.5	0.5	5.3	6.8	8.3	5.0	7.4	2.0	4.3	2.2	5.2	4.5	3.0
Eu	0.53	0.85	0.68	0.86	1.17	0.74	1.11	0.71	0.23	0.19	0.53	0.28	0.57	0.24	0.21	0.10	0.14	0.32	0.30	0.42	1.13	0.71	0.67	0.47	0.93	0.68	0.44	0.72	0.97	0.70	0.43
Gd	0.4	1.3	1.4	1.7	2.3	0.9	2.4	1.7	2.1	1.9	4.0	2.1	4.8	1.9	1.9	0.5	0.7	2.2	1.9	0.4	4.0	5.4	6.5	3.9	5.8	1.6	3.4	1.7	4.1	3.4	1.9
Tb	0.05	0.15	0.22	0.26	0.27	0.08	0.22	0.20	0.30	0.27	0.46	0.33	0.65	0.25	0.28	0.07	0.10	0.29	0.21	0.04	0.35	0.56	0.75	0.48	0.60	0.17	0.39	0.18	0.43	0.32	0.22
Dy	0.26	0.72	1.31	1.50	1.19	0.27	0.79	0.97	1.50	1.31	1.81	1.98	2.69	1.22	1.61	0.39	0.49	1.32	0.86	0.17	1.28	1.94	2.63	1.89	2.09	0.68	1.71	0.75	1.67	1.08	0.96
Ho	0.03	0.15	0.29	0.31	0.20	0.05	0.12	0.16	0.27	0.22	0.28	0.40	0.47	0.21	0.33	0.07	0.10	0.20	0.14	0.03	0.21	0.26	0.39	0.28	0.31	0.11	0.25	0.12	0.29	0.16	0.13
Er	0.07	0.37	0.86	0.83	0.54	0.11	0.35	0.34	0.66	0.59	0.67	1.09	1.11	0.48	0.90	0.17	0.24	0.43	0.33	0.07	0.45	0.59	0.91	0.61	0.78	0.24	0.49	0.32	0.81	0.42	0.32
Tm	0.01	0.06	0.14	0.13	0.07	0.01	0.04	0.04	0.10	0.11	0.08	0.18	0.16	0.07	0.15	0.02	0.04	0.06	0.04	0.01	0.04	0.05	0.08	0.07	0.09	0.03	0.06	0.04	0.11	0.05	0.04
Yb	0.03	0.35	0.89	0.79	0.44	0.06	0.21	0.23	0.58	0.64	0.52	1.22	0.87	0.43	0.98	0.16	0.22	0.36	0.21	0.04	0.25	0.32	0.44	0.41	0.53	0.17	0.35	0.22	0.72	0.26	0.24
Lu	0.01	0.06	0.14	0.12	0.06	0.01	0.03	0.03	0.09	0.08	0.07	0.20	0.12	0.07	0.15	0.02	0.03	0.06	0.03	0.01	0.03	0.03	0.05	0.05	0.07	0.01	0.05	0.03	0.11	0.03	0.04

Table 2 Major (wt %) and trace element (ppm) data of granitoids from the Dzhabyk batholith. Total Fe as FeO*.

	Dzhabyk *s.s.*												Ol'khovsk									Velikopetrovsk					Mochagi						Rodnichki				
Nr.	**588**	**610**	**217**	**962**	**974**	**545**	**972**	**833**	**730**	**515**	**509**	**512**	**581**	**699**	**600**	**911**	**529**	**551**	**525**	**536**	**537**	**641**	**694**	**633**	**650**	**642**	**864**	**398**	**523**	**808**	**800**	**802**	**814**	**820**	**811**	**815**	**740**
SiO_2	75.9	75.0	73.7	73.1	73.0	72.5	72.2	72.0	71.5	71.4	70.7	69.1	75.2	74.6	73.8	73.1	72.5	72.3	71.3	70.5	70.5	74.5	74.3	74.2	73.9	73.3	73.1	72.1	68.7	66.9	64.1	58.0	75.5	69.3	64.8	63.4	58.7
TiO_2	0.07	0.16	0.23	0.20	0.21	0.35	0.21	0.37	0.30	0.25	0.46	0.60	0.12	0.28	0.12	0.24	0.23	0.36	0.37	0.33	0.39	0.18	0.18	0.20	0.18	0.18	0.20	0.30	0.43	0.56	0.75	1.25	0.13	0.48	0.62	0.77	1.14
Al_2O_3	13.5	14.1	14.7	15.0	14.9	15.1	15.3	14.7	14.5	14.9	14.6	14.9	13.2	13.8	14.0	14.2	13.8	13.4	15.0	15.0	14.6	14.0	14.4	13.7	13.8	13.8	14.2	14.2	15.1	14.9	16.3	16.1	12.2	14.0	14.0	16.3	17.0
FeO*	1.63	1.65	1.67	1.76	1.17	1.62	1.56	2.05	2.37	1.64	2.30	3.58	1.58	1.56	1.58	1.86	1.80	2.05	2.05	2.19	2.40	1.87	2.19	2.56	3.14	2.51	1.64	2.21	3.19	3.67	4.52	6.16	2.17	3.43	7.33	4.31	6.24
MgO	0.17	0.22	0.48	0.55	0.72	0.70	0.72	0.60	0.75	0.54	0.72	1.28	0.27	0.39	0.30	0.35	0.55	0.62	0.80	0.90	0.97	0.30	0.62	0.52	0.54	0.50	0.10	0.61	1.11	1.47	1.47	4.10	0.42	0.94	1.26	2.52	3.72
MnO	0.02	0.03	0.03	0.04	0.03	0.02	0.02	0.02	0.03	0.02	0.02	0.07	0.03	0.05	0.04	0.04	0.05	0.05	0.05	0.05	0.05	0.05	0.09	0.09	0.09	0.06	0.02	0.02	0.05	0.04	0.05	0.10	0.02	0.02	0.04	0.07	0.08
CaO	0.62	0.66	1.28	1.09	1.19	1.51	0.98	1.66	1.39	1.26	1.67	1.85	0.84	0.83	0.78	0.98	0.86	1.07	1.11	1.19	1.16	1.00	1.49	1.34	1.42	1.52	0.70	0.88	1.68	2.82	3.51	4.97	1.02	1.75	2.82	3.07	3.27
Na_2O	3.06	3.00	3.30	3.42	3.49	4.08	3.36	3.33	3.87	4.16	3.85	4.53	3.51	3.69	3.70	3.65	3.40	3.63	3.20	3.70	3.66	3.56	3.62	3.44	3.78	3.45	3.81	4.00	3.81	4.24	4.33	4.26	3.06	3.61	4.64	3.50	4.62
K_2O	5.15	4.50	4.57	4.96	4.78	4.53	4.51	4.50	4.69	4.80	5.00	2.95	5.23	4.76	5.23	4.85	5.35	5.42	5.74	5.77	5.61	4.72	3.83	4.56	3.61	4.46	5.61	4.92	4.96	4.87	4.17	3.76	4.88	5.91	3.04	4.61	3.56
P_2O_5	0.05	0.05	0.06	0.10	0.11	0.08	0.09	0.08	0.09	0.08	0.09	0.15	0.03	0.09	0.04	0.06	0.06	0.08	0.08	0.13	0.14	0.07	0.09	0.07	0.09	0.06	0.11	0.16	0.19	0.23	0.19	0.23	0.01	0.04	0.15	0.24	0.41
Total	100.1	99.4	100.0	100.1	99.6	100.4	98.9	99.3	99.4	99.0	99.4	99.0	100.0	100.0	99.6	99.3	98.6	99.0	99.7	99.8	99.5	100.3	100.4	100.5	100.6	99.8	99.5	99.5	99.2	99.6	99.4	98.9	99.3	99.5	98.8	98.7	98.7
Li	34	27	34	42	32	40	35	40	39	25	40	62	22	68	37	43	62	31	48	42	44	26	28	44	42	44	7	12	19	16	15	24	5	10	15	25	16
Rb	235	189	122	167	139	183	157	148	194	119	85	85	217	288	192	198	241	217	192	219	240	175	185	164	180	157	147	162	101	108	92	119	96	109	67	124	87
Cs	5.4	3.8	5.6	5.4	1.9	3.3	2.9	2.9	4.1	2.4	3.0	5.2	4.2	7.2	7.0	6.0	5.4	2.5	2.9	4.4	3.4	5.0	6.7	16	15.6	9.6	1.1	3.0	3.0	1.2	1.8	1.7	1.4	1.2	1.7	1.9	1.8
Be	3.3	3.8	2.8	2.8	2.3	2.2	2.7	1.8	1.6	2.6	2.6	4.6	4.7	4.2	3.9	5.1	4.5	2.7	3.0	4.2	2.7	4.1	3.2	4.8	6.2	4.4	1.9	2.2	2.1	1.6	3.4	1.9	1.4	1.1	2.7	1.6	2.3
Sr	62	74	119	140	157	317	203	277	246	167	188	216	39	94	88	89	82	155	101	196	172	107	134	124	131	168	233	292	475	618	567	841	234	618	861	603	914
Ba	253	298	508	601	556	1113	749	910	1151	841	1017	771	169	419	360	348	341	472	331	789	761	476	429	367	352	465	461	596	912	1115	1003	1237	1115	1926	1655	1409	1472
Sc	1.9	3.3	2.7	2.7	2.3	3.5	2.6	3.1	3.7	1.6	2.9	5.7	2.7	4.7	3.1	3.1	4.7	3.9	3.7	8.7	5.8	6.1	4.0	8.7	7.6	8.3	2.0	3.2	4.8	4.8	10.3	17	6.1	3.6	10	10	14
V	6	10	17	13	11	21	18	22	23	17	30	40	8	13	7	14	14	21	15	21	24	9	16	20	16	21	13	20	45	47	64	127	12	41	51	75	120
Co	0.1	0.2	0.9	1.3	1.2	2.8	1.7	2.1	3.0	0.1	1.8	2.8	0.0	3.0	0.1	0.4	1.1	1.8	3.1	3.3	3.7	2.0	3.0	3.2	3.0	2.8	2.3	3.4	5.4	5.8	8	17	1.7	2.9	6.2	10	14
Zn	19	27	48	42	45	56	54	65	58	43	72	92	19	40	26	32	48	36	52	43	52	16	38	30	34	24	27	33	56	66	52	96	14	64	58	114	93
Ga	15	17	16	18	17	20	19	18	18	17	18	23	16	18	16	17	18	17	18	19	18	14	15	16	16	17	16	17	17	18	18	18	13	17	17	20	21
Y	2.3	5.9	7.7	4.7	3.9	5.4	5.0	5.2	5.2	3.3	3.5	6.3	5.9	16	9.1	6.7	5.9	16	13	16	20	9.4	10	12	14	15.6	5.6	13	10	10	12	18	5.0	4.9	17	16	12
Nb	13	22	13	11	9.2	8.6	10	7.4	7.9	5.5	8.8	21	39	30	16	25	27	28	25	21	29	6.9	12	13	11	10	15	14	21	16	24	18	5.1	6.1	9.1	24	13
Ta	1.3	2.0	1.3	1.3	0.7	0.6	0.8	0.5	0.6	0.6	0.9	1.7	3.2	3.1	2.2	2.0	2.7	2.3	2.3	1.7	2.6	1.6	1.4	2.5	2.8	1.7	1.4	0.9	1.6	1.1	2.0	0.9	0.5	0.2	0.6	1.7	0.6
Zr	51	92	143	137	112	176	143	173	164	140	184	231	104	144	97	131	110	185	109	127	177	61	70	76	73	78	92	112	126	153	165	131	56	178	193	188	78
Hf	1.6	3.2	4.1	4.0	3.4	5.0	4.1	4.7	4.7	4.2	4.9	6.1	3.8	4.7	3.3	4.1	3.5	5.9	3.2	3.2	5.2	2.0	2.4	2.2	2.2	2.3	2.8	3.5	3.5	4.2	3.8	2.4	1.7	4.5	4.3	4.6	1.6
Pb	32	32	27	30	33	33	30	31	31	32	28	28	37	29	36	33	30	31	24	26	28	21	26	21	21	21	32	38	28	29	20	17	23	28	21	23	18
U	2.6	4.2	6.6	1.7	2.9	8.3	1.9	2.1	2.8	2.0	2.4	1.6	7.6	5.5	2.7	4.7	4.3	4.1	3.1	2.3	4.3	1.7	1.9	2.8	3.4	2.1	4.1	3.6	3.9	3.4	2.3	1.5	1.7	2.9	1.9	3.2	1.6
Th	8	15	22	22	18	14	19	22	21	16	12	10	14	20	25	22	23	29	25	14	18	5.6	12	8.8	8.6	7.7	27	23	20	16	13	23	9.3	19	14	17	8.4
La	4.6	7.6	21	22	21	28	26	33	37	20	25	20	6.9	35	20	15	8.8	47	20	33	36	7.6	23	17	16	20	35	40	58	55	52	98	26	80	58	53	48
Ce	9.0	23	44	47	45	52	54	66	69	47	51	44	21	65	42	36	23	100	45	67	84	20	48	35	36	39	69	76	118	120	105	204	52	144	118	116	93
Pr	0.9	1.7	4.4	4.6	4.6	5.1	5.5	6.6	6.9	4.4	5.1	4.3	1.6	7.1	4.0	2.8	1.9	8.7	4.1	6.7	8.1	1.6	4.9	3.6	3.5	4.3	6.7	7.3	12	12	11	19	4.8	14	12	12	10
Nd	2.9	5.9	15	15	15	17	18	22	23	15	14	14	5.8	23	13	8.9	6.4	28	15	22	29	5.6	17	12	12	15	21	23	41	40	34	63	15	42	38	43	36
Sm	0.6	1.2	2.8	2.5	2.6	2.5	2.8	3.3	3.2	2.4	2.2	2.2	1.3	4.0	2.4	1.5	1.4	4.5	3.2	3.8	4.9	1.2	3.2	2.5	2.6	3.2	3.0	3.4	6.0	5.9	5.0	9.1	2.0	4.8	5.5	6.8	5.7
Eu	0.16	0.18	0.37	0.29	0.28	0.42	0.36	0.46	0.46	0.37	0.43	0.43	0.13	0.49	0.28	0.26	0.23	0.63	0.37	0.79	0.71	0.21	0.35	0.36	0.36	0.45	0.47	0.65	1.1	1.2	1.1	2.0	0.68	0.7	1.4	1.4	1.4
Gd	0.6	1.0	2.1	1.7	1.7	1.8	1.8	2.1	2.1	1.7	1.6	1.7	1.1	3.2	2.1	1.3	1.2	3.6	2.4	3.2	3.9	1.2	2.6	2.5	2.4	2.9	1.9	2.2	3.6	3.5	3.8	6.7	1.3	2.5	4.1	4.8	4.5
Tb	0.09	0.18	0.30	0.23	0.20	0.22	0.25	0.25	0.25	0.18	0.18	0.23	0.18	0.48	0.30	0.20	0.18	0.50	0.39	0.49	0.60	0.21	0.40	0.36	0.36	0.44	0.25	0.38	0.48	0.45	0.49	0.77	0.16	0.27	0.53	0.65	0.51
Dy	0.5	1.2	1.6	1.1	0.9	1.3	1.2	1.1	1.2	0.8	0.8	1.3	1.2	2.9	1.7	1.1	1.1	3.0	2.6	2.6	3.6	1.4	2.2	2.1	2.2	2.6	1.4	2.3	2.3	2.2	2.2	3.4	0.8	1.2	2.8	3.5	2.3
Ho	0.12	0.25	0.32	0.22	0.16	0.23	0.21	0.20	0.21	0.14	0.16	0.25	0.30	0.59	0.34	0.26	0.24	0.60	0.54	0.56	0.75	0.32	0.40	0.44	0.49	0.58	0.25	0.45	0.41	0.39	0.42	0.65	0.16	0.20	0.57	0.61	0.41
Er	0.32	0.79	0.82	0.54	0.40	0.60	0.49	0.53	0.51	0.40	0.46	0.70	0.9	1.7	1.0	0.8	0.7	1.8	1.5	1.6	2.1	1.0	1.2	1.3	1.4	1.58	0.71	1.3	1.1	1.1	1.1	1.5	0.44	0.6	1.6	1.7	1.0
Tm	0.06	0.15	0.14	0.08	0.06	0.09	0.07	0.08	0.08	0.06	0.07	0.11	0.18	0.28	0.17	0.16	0.13	0.28	0.23	0.26	0.34	0.16	0.19	0.20	0.23	0.24	0.10	0.21	0.15	0.14	0.16	0.22	0.07	0.09	0.24	0.24	0.15
Yb	0.38	1.03	0.90	0.49	0.38	0.59	0.45	0.49	0.56	0.41	0.44	0.69	1.3	1.9	1.1	1.1	0.9	1.9	1.3	1.7	2.3	1.2	1.3	1.3	1.6	1.62	0.65	1.2	1.1	0.94	1.0	1.4	0.52	0.6	1.5	1.5	0.91
Lu	0.06	0.18	0.14	0.08	0.05	0.10	0.06	0.08	0.09	0.07	0.07	0.11	0.22	0.32	0.19	0.19	0.16	0.33	0.21	0.26	0.36	0.21	0.22	0.22	0.25	0.26	0.09	0.20	0.15	0.15	0.17	0.20	0.09	0.11	0.23	0.23	0.14

Table 3 Sr and Nd whole-rock isotopic data for Murzinka and Dzhabyk granitoids

Sample		Rb (ppm)	Sr (ppm)	$^{87}Rb/^{86}Sr$	$^{87}Sr/^{86}Sr$ Measurement[a]	$^{87}Sr/^{86}Sr$ Initial[b]	Sm (ppm)	Nd (ppm)	$^{147}Sm/^{144}Nd$	$^{143}Nd/^{144}Nd$ Measurement[a]	$^{143}Nd/^{144}Nd$ Initial[b]	εNd Initial[b]	T_{DM}[c] (Ma)
Murzinka batholith (Y, V, M=Yuzhakovsk, Vatikha, Murzinka s.s.)													
129	Y	26.5	519	0.1476	0.70470	0.70416	1.80	10.63	0.1026	0.512692	0.512521	+4.1	707
42	M	168	250	1.949	0.71166	0.70459	0.92	4.89	0.1142	0.512659	0.512468	+3.1	758
51	M	123	288	1.234	0.70997	0.70549	0.54	2.65	0.1227	0.512634	0.512429	+2.3	796
50	M	210	106	5.725	0.72496	0.70419	2.87	15.92	0.1088	0.512359	0.512177	−2.6	1218
22	M	214	73	8.523	0.73540	0.70447	3.07	15.89	0.1169	0.512048	0.511853	−8.9	1694
115	Y	124	409	0.8803	0.71241	0.70922	2.80	17.69	0.0956	0.512467	0.512307	−0.05	1053
9	V	139	130	2.687	0.71886	0.70912	3.34	21.39	0.0945	0.511942	0.511784	−10.3	1856
61	V	60.6	181	0.9711	0.71275	0.70923	3.02	19.45	0.0938	0.511960	0.511803	−9.9	1829
17	V	164	95.8	4.948	0.72663	0.70868	3.38	16.11	0.1269	0.511911	0.511699	−11.9	1903
Dzhabyk batholith (Dz, Ol, Mo, Ro = Dzhabyk s.s., Oĺkhovsk, Mochagi, Rodnichki)													
972	Dz	158	203	2.258	0.71398	0.70466	2.92	19.22	0.0918	0.512493	0.512319	+1.1	1013
974	Dz	140	166	2.441	0.71380	0.70372	2.46	15.27	0.0974	0.512492	0.512307	+0.8	1014
833	Dz	154	270	1.653	0.71098	0.70416	3.96	26.29	0.0911	0.512495	0.512322	+1.1	1010
962	Dz	166	145	3.314	0.71771	0.70404	2.26	14.19	0.0965	0.512528	0.512345	+1.6	959
525	Ol	181	104	5.063	0.72460	0.70370	3.19	15.07	0.1280	0.512564	0.512321	+1.1	904
802	Mo	141	847	0.4833	0.70661	0.70462	9.02	61.25	0.0890	0.512477	0.512308	+0.8	1037
800	Mo	93.7	584	0.4642	0.70650	0.70459	5.90	41.71	0.0855	0.512453	0.512291	+0.5	1074
811	Ro	67.8	878	0.2233	0.70577	0.70485	5.63	39.21	0.0868	0.512469	0.512304	+0.8	1050
814	Ro	95.1	248	1.111	0.71017	0.70559	1.96	15.29	0.0775	0.512412	0.512265	+0.01	1137

[a] measured ratio, $2\sigma_m$ during measurements were <0.004% for $^{87}Sr/^{86}Sr$ and <0.0015% for $^{143}Nd/^{144}Nd$, respectively

[b] Initial ratios were calculated for 255 Ma (Murzinka) and 290 Ma (Dzhabyk), using $\lambda^{187}Rb$=1.42E-11 y^{-1}, $\lambda^{147}Sm$=6.54E-12 y^{-1}, $^{147}Sm/^{144}Nd^0_{Chur}$=0.1966 and $^{143}Nd/^{144}Nd^0_{Chur}$=0.512638

[c] Nd model ages were calculated after Liew and Hofmann (1988), using $^{143}Nd/^{144}Nd_{DM}$=0.513151, $^{147}Sm/^{144}Nd_{DM}$=0.219 and $^{147}Sm/^{144}Nd_{CC}$=0.12

REE have positive Eu anomalies and decrease almost continuously from La to Sm and from Gd to Lu. Samples with high total REE have negative Eu anomalies, decrease from La to Sm and from Gd to Ho–Er and then become nearly flat for the heaviest HREE. The LREE/HREE ratio is always elevated, with La_N/Yb_N ~48–202.

Murzinka s.s. granites have the highest concentrations of Li, Rb, Cs, Be, Ga, Y, U and Nb, and the lowest values of K/Rb (128–214, average 162) and Th/U (~4.5). Sr and Ba contents vary largely and correlate negatively with the Rb/Sr ratio. The Nd/Th ratios are very low (~1) and less variable than in the Vatikha and Yuzhakovsk granites. Chondrite-normalised REE patterns have moderate La_N/Yb_N ratios (6–59, average ~24), invariably negative Eu anomalies, and flat profiles for the heaviest HREE. The LREE, HREE, Y, Nb and Ga contents commonly correlate positively with the Rb/Sr ratio, whereas Zn and V correlate negatively with it.

The Dzhabyk batholith

Dzhabyk granitoids are also highly heterogeneous (Table 2). Two groups are distinguished geochemically, one comprising the Dzhabyk s.s., Ol'khovsk and Velikopetrovsk units, hereafter generically called the "granites", and the other consisting of the Rodnichki and Mochagi units, hereafter called the "quartz-monzonites". The first group is volumetrically much more important, formed of peraluminous granites with SiO_2 commonly in the range 69–76% and $K_2O>Na_2O$ (Fig. 2). The second is formed mainly of metaluminous to slightly peraluminous quartz-monzonites, quartz-monzodiorites, syenogranites and minor leucogranites, characterised by high total alkali contents (Fig. 2).

Dzhabyk granites are slightly richer in Ti, Mg, Fe, Ca, Li, Rb, Ga, Nb, V and HREE, but have comparable LREE, Sr and Ba contents to similar rocks of the Murzinka batholith and the same fairly constant Sr/Ba ratio (average ~0.29). The MgO, FeO_{tot} and CaO contents are, however, generally below 0.8, 3.5 and 1.8 wt.%, respectively. The Rb/Sr ratio is typically ~1 but commonly decreases with the concentration of Ca from a high of 3.8 to a low of 0.4. Th/U ratios are in the range of ~2–10 and never reach the elevated values characteristic of the Vatikha granites. Nd/Th ratios can be very low (Fig. 3), with an average value close to unity. Chondrite-normalised REE patterns (Fig. 5) show a smooth decrease from La to Sm, a negative Eu anomaly (Fig. 4), more intense in the case of the Ol'khovsk and Velikopetrovsk granites, and a flat or positive slope from Gd to Lu. They have a moderate La_N/Yb_N of 8–45, comparable to that of Murzinka s.s. granites.

Dzhabyk quartz-monzonites have a distinctive geochemistry with respect to the granites. They have lower concentrations of Li, Rb and Cs, higher concen-

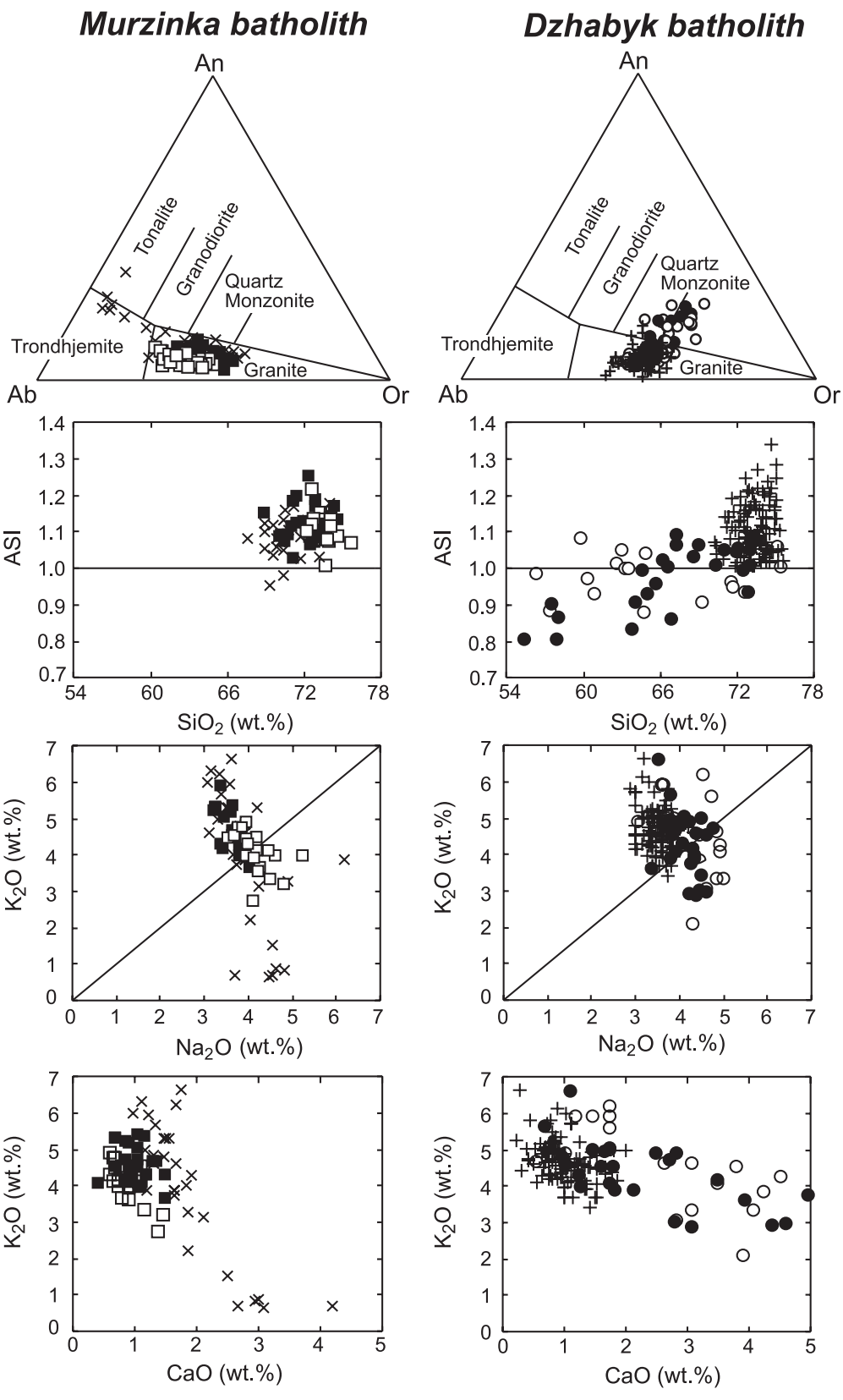

Fig. 2 Or–Ab–An plot (fields after Barker 1979) and major element variation diagrams for granitoids from the Murzinka and Dzhabyk batholiths. Note that the classification of the rocks in the text were done by modal content. Murzinka: Yuzhakovsk (*crosses*), Vatikha (*black squares*), Murzinka (*open squares*); Dzhabyk: granites (*pluses*) and quartz-monzonites from Rodnichki (*circles*) and Mochagi (*black dots*)

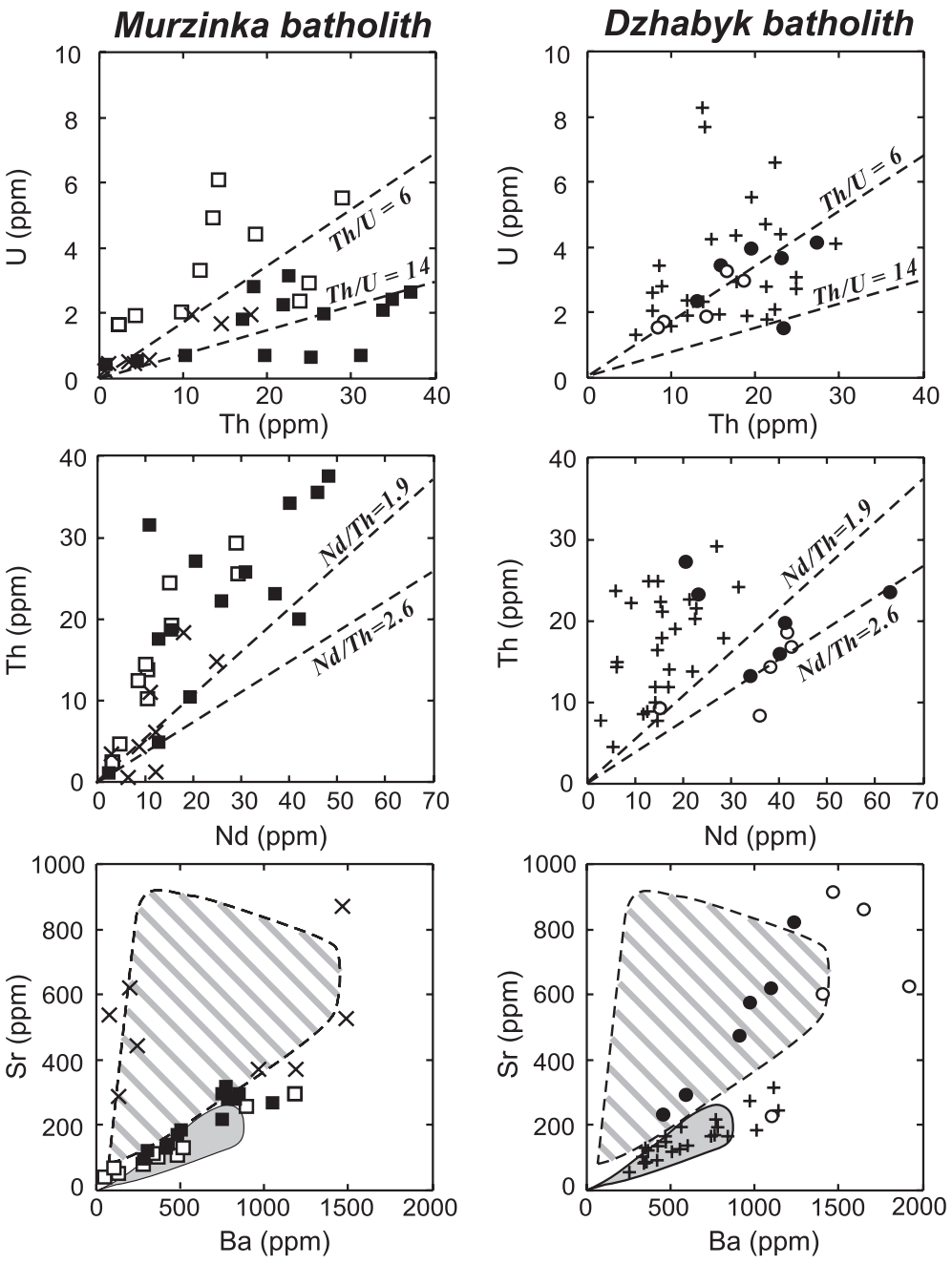

Fig. 3 U vs Th, Th vs Nd and Sr vs Ba diagrams for granitoids from the Murzinka and Dzhabyk batholiths. Symbols as in Fig. 2. For comparison, the reference lines for amphibolite-facies (Th/U=6) and granulite-facies (Th/U=14) rocks of the Ivrea-Verbano zone and Iberian peraluminous granites (Nd/Th=1.9) and Ivrea-Verbano granites and metapelites (Nd/Th=2.6; Bea and Montero 1999; Bea et al. 1999). *Shaded field:* Iberian peraluminous granites (Bea et al. 1999). *Striped field:* metaluminous subduction-related granitoids from the Verkhisetsk batholith (Bea et al. 1997)

trations of LREE (ΣLREE ~100–400 ppm), Ba and Sr, lower Rb/Sr and higher Sr/Ba, Zr/Hf and Nd/Th ratios. The chondrite-normalised REE patterns are also different (Fig. 5). Quartz-monzonites usually have higher LREE/HREE ratios, with $La_N/Yb_N>25$ and a moderate negative or a marked positive Eu anomaly. The LREE, HREE and elements, such as Ba, Sr, Ga, Sc, V, Co and Zn, show, particularly for the Mochagi samples, a clear negative correlation with the silica content, and only the Pb, U and Th concentrations correlate positively with SiO_2.

Sr- and Nd-isotope geology

Murzinka granitoids

On the $^{87}Sr/^{86}Sr$ vs $^{87}Rb/^{86}Sr$ diagram (Fig. 6), Murzinka rocks plot within two parallel regression lines, which yield ages of 248±6 and 259±8 Ma, consistent with the single-zircon age of 254±5 Ma (Montero et al. 2000). A contemporaneous intrusion is also supported by the field relations. The Vatikha granites and one granitic vein from Yuzhakovsk plot on the upper line, corresponding to an $^{87}Sr/^{86}Sr_{init}$ of 0.7093,

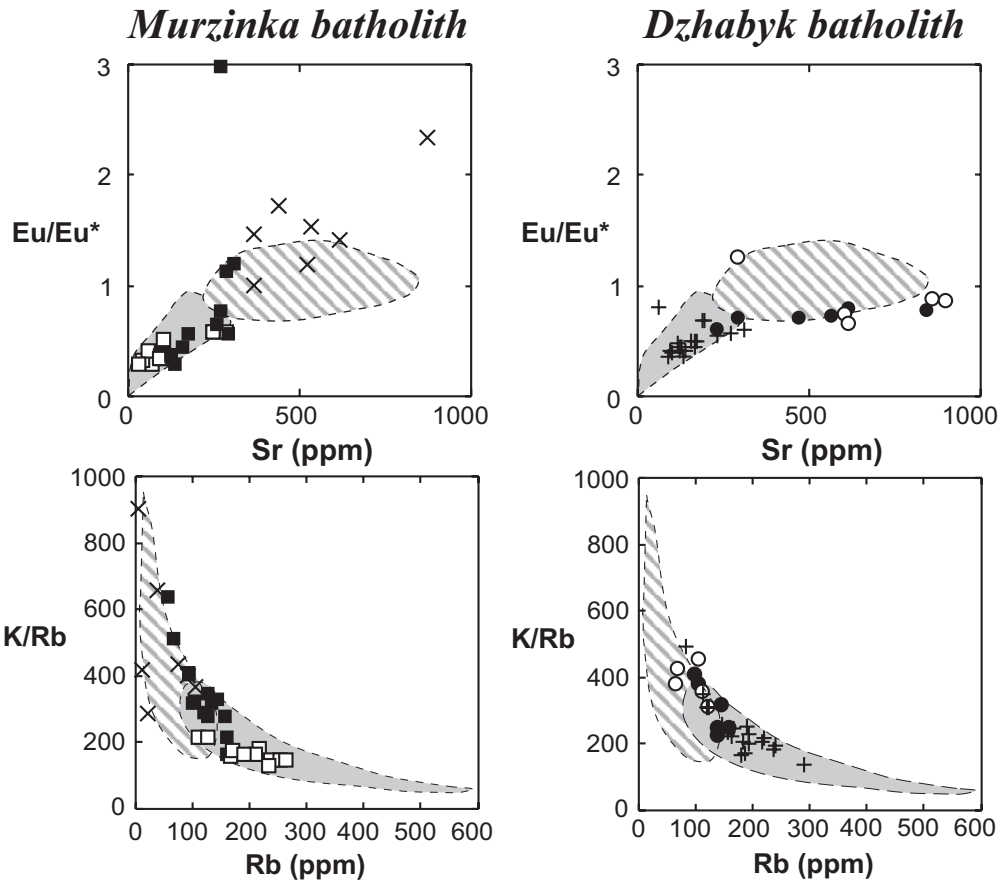

Fig. 4 Eu/Eu* vs Sr and K/Rb vs Rb diagrams for granitoids from the Murzinka and Dzhabyk batholiths. Symbols and fields as in Figs. 2 and 3

whereas the Murzinka s.s. granites and one trondhjemitic vein from Yuzhakovsk plot on the lower line, corresponding to an $^{87}Sr/^{86}Sr_{init}$ of 0.7042. It seems, therefore, that the Murzinka batholith is composed of granitoids with high (HRS) and with low radiogenic Sr (LRS). $^{143}Nd/^{144}Nd_{init}$ (Table 3) are highly variable; as in Murzinka granites the εNd_{255} ranges from –8.9 to +3.1 and in Vatikha granites from –9.9 to –11.9. In Yuzhakovsk, the εNd_{255} of the LRS trondhjemitic vein (Y129) is +4.1 and that of the HRS granitic vein (Y115) is +0.05. Calculated Nd model ages (Liew and Hofmann 1988), which give an estimate of the average crustal residence time of the REE in granite protoliths, are in the range of ~1050–1900 and ~700–1700 Ma for the HRS and LRS granites, respectively (Table 3).

Dzhabyk granitoids

On the Rb–Sr isochron diagram (Fig. 6), Dzhabyk rocks, similarly to the Murzinka rocks, also plot along two different correlation lines with a slope corresponding to ~290 Ma, in good agreement with the single zircon age of 291±4 Ma (Montero et al. 2000). The quartz-monzonites and one sample of the Dzhabyk granites define the upper line, with $^{87}Sr/^{86}Sr_{init}$ ~0.7049. In this case, the small dispersion on the horizontal axis and the considerable scattering do not allow an age calculation. The second line is defined by the granites and corresponds to an age of 282±17 Ma with a $^{87}Sr/^{86}Sr_{init}$ of 0.7043. The difference in the $^{87}Sr/^{86}Sr_{init}$ between these two groups is notably less marked than in the case of Murzinka. Nd isotopes are very similar in both rock types (Table 3): the εNd_{290} is always positive and ranges from 0.0 to +0.8 in quartz-monzonites, and from +0.8 to +1.6 in granites. In the εNd_{290} vs 1/Sr plot (Fig. 6) no clear correlation is visible. Calculated Nd model ages are remarkably uniform, clustering around 900–1100 Ma.

Discussion

Uralian continental-type granites have many geochemical features (e.g. $K_2O/Na_2O>1$, ASI ~1.0–1.25, elevated Rb, U, Th and LREE and low Sr/Ba ratios) that clearly differentiate them from West Uralian subduction-related granitoids, formed by partial melting of an oceanic source (e.g. Bea et al. 1997). They are comparable in many regards to certain post-collisional Variscan granitoids of western Europe that were produced predominantly by crustal melting (e.g. Finger et al. 1997; Bea et al. 1999; Gerdes et al. 2000).

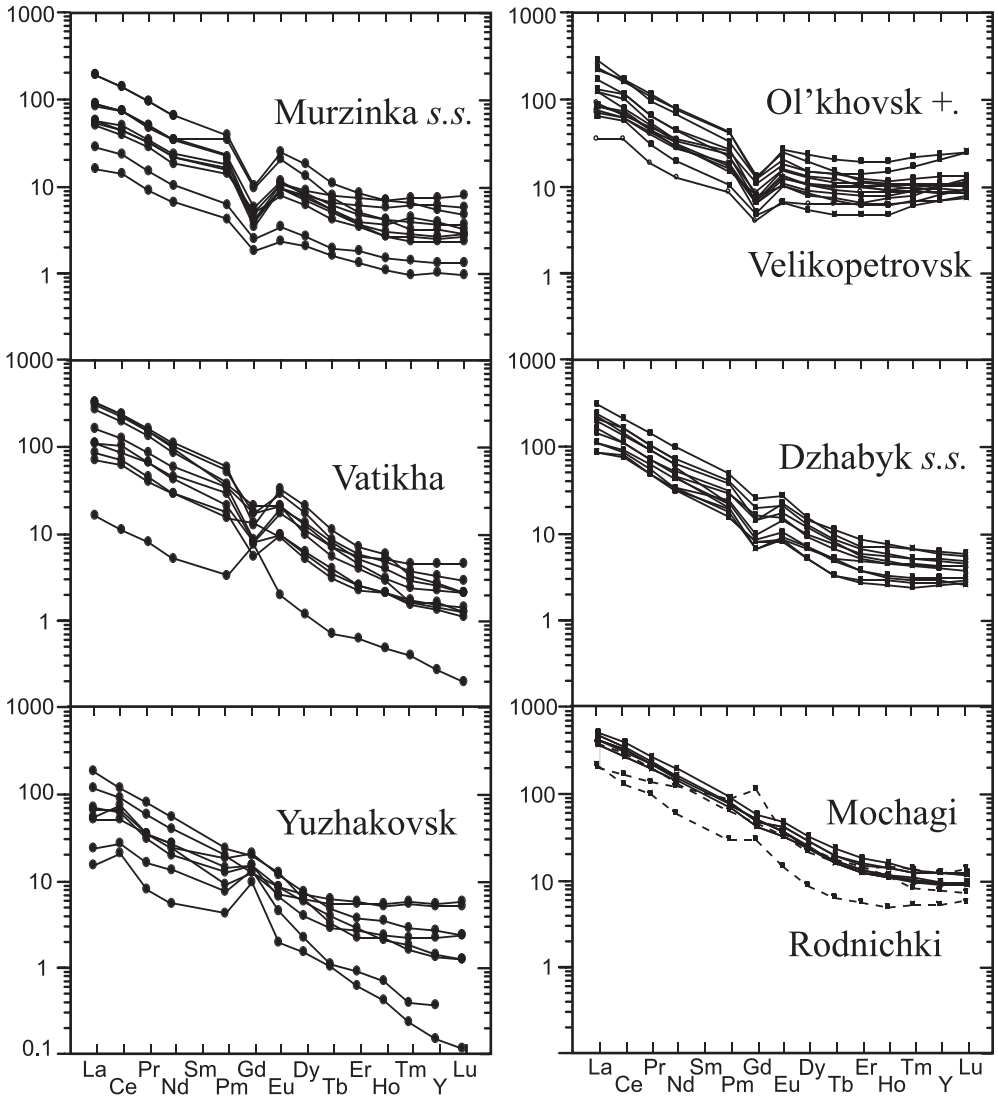

Fig. 5 Chondrite-normalized rare earth element (REE) diagrams for granitoids from the Murzinka and Dzhabyk batholiths

Dzhabyk and Murzinka granitoids were also generated long after ocean closure in a post-collisional setting. In contrast to Variscan granites, which had sources with a long crustal residence time (Fig. 7), the Sr- and Nd-isotope data presented suggest significant amounts of juvenile material in the generation of the East Uralian granitoids.

Petrogenesis of Murzinka granitoids

The large isotopic variations in Murzinka granitoids can, in theory, be explained by hybridization of mafic mantle-derived magmas with silica-rich melts derived from old crustal sources; however, the scarcity of mafic enclaves, the relatively small compositional variation of the granitoids and their elevated peraluminosity and silica contents argue against such a process. Murzinka s.s. granites, for instance, vary by approximately 12 εNd units with a change in SiO_2 of <2 wt%. Therefore, the involvement of a mantle-derived magma in Murzinka granite genesis either in a mixing process or an assimilation and combined fractional crystallisation process (DePaolo 1981) is regarded as unlikely. An alternative explanation is a purely crustal origin of the magmas with the involvement of protoliths with a large juvenile component. These magmas may be derived from the destruction of a young island arc and would have an isotopic composition almost identical to that of mantle-derived magmas. If these materials were buried quickly and underwent partial melting, the resulting magmas would be felsic and peraluminous and inherit, at the same time, the primitive isotopic composition of their source. Since the Uralian evolution is characterised, in contrast to the Variscides, by the amalgamation of various upper-Paleozoic island arcs (Zonenshain et al. 1990; Fershtater et al. 1997; Puchkov 1997; Brown et al. 1998), and it has been shown that materials from Devonian island arcs have been metamorphosed at granulite-facies con-

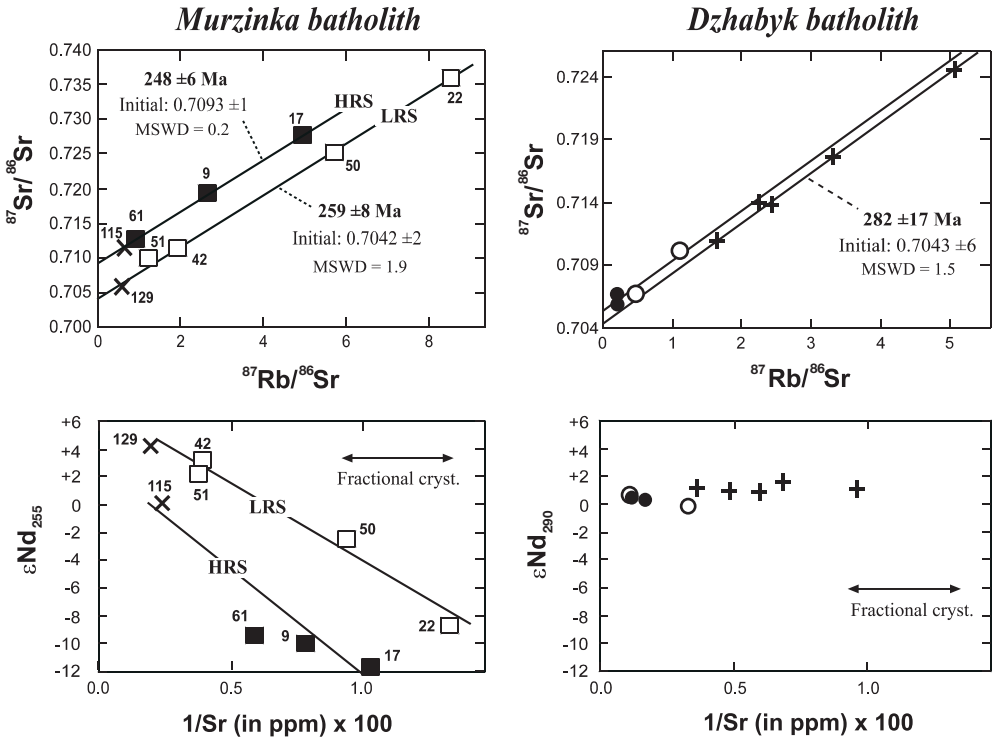

Fig. 6 $^{87}Sr/^{86}Sr$ vs $^{87}Rb/^{86}Sr$ and εNd_{init} vs 1/Sr plots of Murzinka and Dzhabyk granitoids. Symbols as in Fig. 2. Sample numbers shown for Murzinka granitoids near symbols. Rb/Sr ages were calculated using linear least-squares regression (York 1969) with MSWD after Wendt (1986). Errors were calculated using the algorithm of Titterington and Halliday (1979) with 2σ errors for $^{87}Rb/^{86}Sr$=1.2% and $^{87}Sr/^{86}Sr$=0.005%. Sample 51 deviates from a linear trend and was not used for the isochron calculation. See text for further explanation

ditions (Friberg et al. 2000), we tentatively suggest that they represent the source materials for the East Uralian granitoids.

The compositional differences of partial melts produced from crustal sources, such as amphibolites, tonalitic gneisses, metagreywackes and metapelites, can be visualised well in the $Al_2O_3/(MgO+FeO_{tot})$ vs $CaO/(MgO+FeO_{tot})$ diagram (Fig. 8; Gerdes 1997; Gerdes et al. 2000). The major element composition and variation of Murzinka s.s. and Vatikha granites are very similar to experimental melts of metagreywackes (e.g. Conrad et al. 1988; Montel and Vielzeuf 1997). Melts derived from meta-igneous sources are metaluminous to peraluminous and have higher CaO

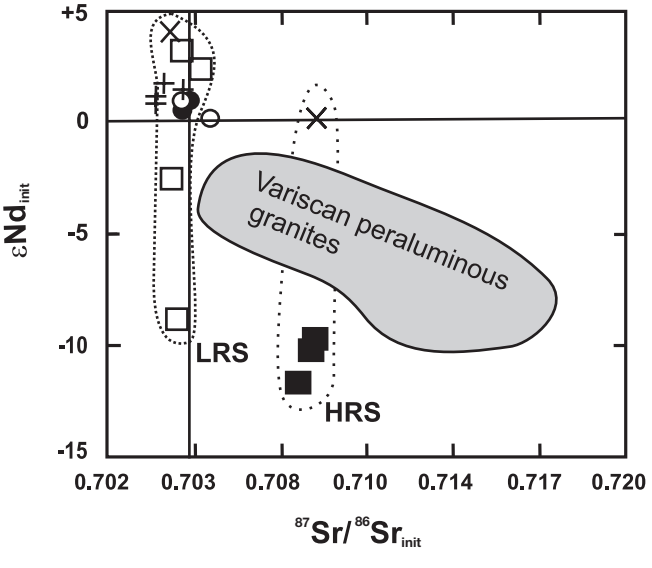

Fig. 7 εNd_{init} vs $^{87}Sr/^{86}Sr_{init}$ of Murzinka and Dzhabyk granitoids. Symbols as in Fig. 2. The field of Variscan peraluminous granitoids is shown for comparison (Pin and Duthou 1990; Gerdes et al. 1998; Bea et al. 1999)

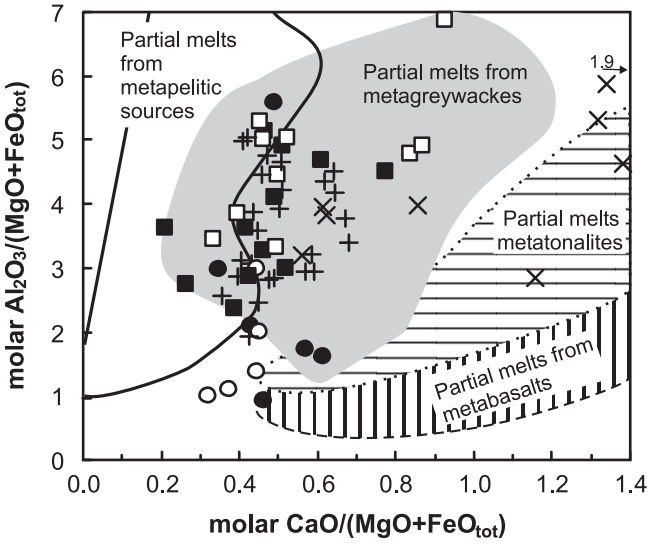

Fig. 8 $Al_2O_3/(MgO+FeO_{tot})$ vs $CaO/(MgO+FeO_{tot})$ plot for the Murzinka and Dzhabyk granitoids. *Outlined fields* are for water-undersaturated partial melts (>9 vol.%) derived from different protoliths under crustal P–T conditions (0.5–1.5 GPa, 725–1000 °C). Modified after Gerdes (1997). See Gerdes et al. (2000) for references

and lower K_2O than granites from Murzinka. Partial melts of metapelites are more peraluminous (ASI>1.2) than East Uralian granites and usually have lower Na_2O and CaO (Vielzeuf and Holloway 1988; Patiño-Douce et al. 1990).

Trace element and Sr isotopic composition suggest that Murzinka and Vatikha granites were generated at different melting conditions and from distinct sources, one with predominantly high $^{87}Sr/^{86}Sr_{init}$ (HRS) and the other with predominantly low $^{87}Sr/^{86}Sr_{init}$ (LRS). Vatikha granites are typified by elevated LREE/HREE ratios and high K/Rb and Th/U, similar to partial melts derived from granulite-grade metasediments (e.g. Bea and Montero 1999). High $^{87}Sr/^{86}Sr_{init}$ with high Ba and Sr contents and moderate Rb/Sr imply an old relatively feldspar-rich protolith and a residue relatively poor in K-feldspar or biotite. We therefore propose that Vatikha granites were produced in the granulite facies of a probable greywacke source with a long crustal residence, leaving a residuum rich in garnet. The moderate La_N/Yb_N of Murzinka s.s. granites, however, indicates that garnet was not a major phase in the residuum and their K/Rb and Th/U contrast sharply with those of the Vatikha granites. The primitive Sr isotopic composition implies a young protolith probably rich in juvenile detritus derived from upper-Paleozoic island arcs. In Fig. 9 we test the hypotheses that Vatikha and Murzinka s.s. granites were generated at different P–T conditions from a metagreywacke source. We model trace element contents using a batch-melting equation (Hanson 1978), different restite assemblages at 25–42 vol.% partial melting (Conrad et al. 1988), a Phanerozoic greywacke as starting material (Taylor and McLennan 1985) and a range of mineral/melt partition coefficients for felsic rocks (Rollinson 1993). Except perhaps for the LREE, the average trace element composition of Murzinka s.s. granites agrees very well with the compositions calculated using an amphibolite-facies residue (C 1; Fig. 9). Restitic monazite was not considered but is very likely at these temperatures and would cause lower LREE concentrations in the calculated melts. The composition of Vatikha granites are in accordance with a granulite-facies model (C 2). In contrast, melts derived from metapelites would have stronger HREE depletion because of higher restitic garnet contents (Vielzeuf and Holloway 1988).

Petrographic observations provide additional information for distinct melting conditions. Vatikha granites have antiperthitic plagioclase and orthoclase of the lowest triclinicity, indicating crystallisation at high temperatures from a water-poor melt. Murzinka s.s. granites, in contrast, have non-perthitic plagioclase and microcline of the highest triclinicity, which, together with the abundance of pegmatites, suggests they crystallised at lower temperatures from a water-rich magma.

The element correlations in Vatikha and Murzinka s.s. granites are not always well defined. Considerable

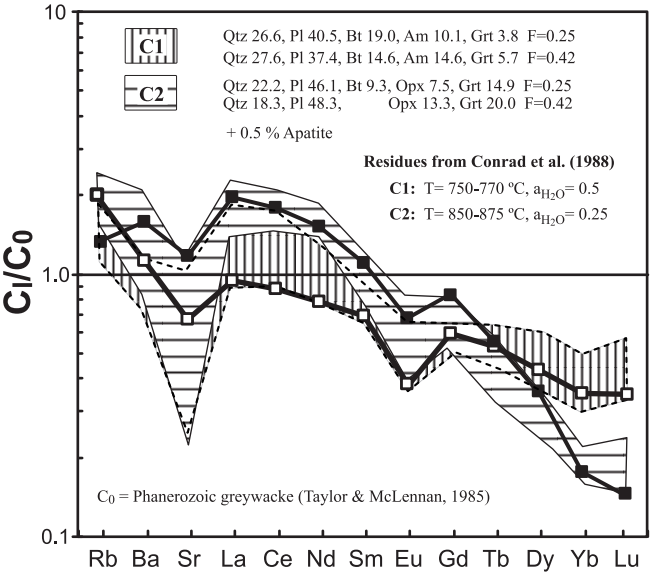

Fig. 9 Average trace element concentration of Murzinka s.s. and Vatikha granites (C_l) in comparison with calculated composition of partial melts in equilibrium with granulite-facies and amphibolite-facies residues. Residues (C1 and C2) are derived from melting experiments on greywackes by Conrad et al. (1988) at 1 GPa. Assumed protolith concentration (C_0) is from average Phanerozoic quartz-intermediate greywacke (Taylor and McLennan 1985). Mineral/melt partition coefficients are from Rollinson (1993, Table 4.3). See text for further explanation. *Qtz* quartz; *Plag* plagioclase; *Bt* biotite; *Am* amphibole; *Grt* garnet

variation in different trace elements and less so in major elements in both granite types can be explained by fractional crystallisation, melting of a heterogeneous source, or a combination of both processes. The highly variable εNd_{255} in Murzinka s.s. granites show a clear correlation with the Rb/Sr ratio and also to inverse element contents, e.g. of V, Ba, Sr and of all major elements except iron. The trondhjemitic vein (Y129) is frequently situated along these trends. These unusual, but well-defined, correlations of the LRS granitoids are clearly revealed, e.g. in the εNd_{255} vs 1/Sr plot (Fig. 6), and most likely represent mixing lines. For several trace elements, particularly for the LREE, these correlations are only badly defined or non-existent and therefore do not support a simple magma mixing process. It is more likely that these trends in LRS granitoids are related to a heterogeneous source, and that the initial magma composition changed due to fractional crystallisation and incomplete homogenisation during ascent and emplacement. The Rb/Sr vs $K_2O/(CaO+Na_2O)$ diagram can be used to visualise the effect of major-mineral fractionation on magma composition (Fig. 10); thus, some variation in LRS granitoids can be explained by plagioclase, biotite and K-feldspar fractionation. The very low Rb/Sr, Ba and K of the trondhjemitic veins suggest high biotite fractionation or, more likely, a residue rich in biotite. High Ca, Sr and positive Eu anomalies point to high proportions of plagioclase in the melt, proba-

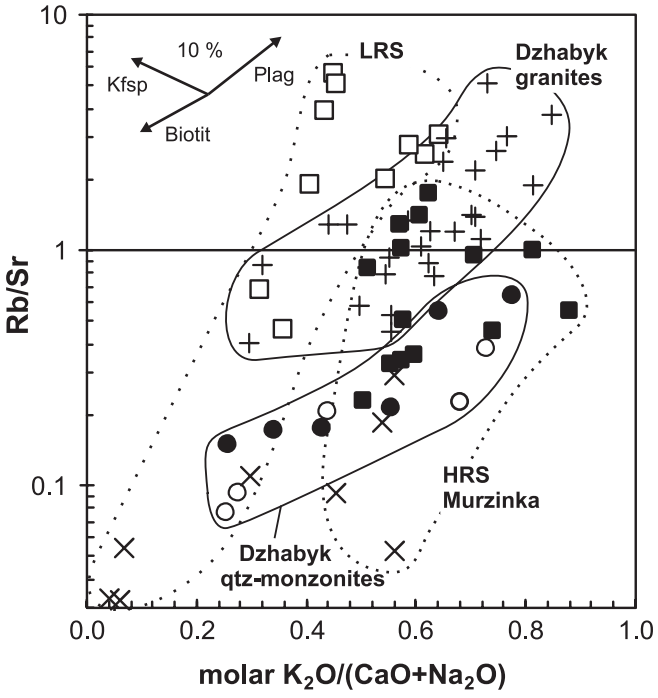

Fig. 10 Rb/Sr vs $K_2O/(CaO+Na_2O)$ plot for Murzinka and Dzhabyk granitoids. *Arrows* show change in melt composition after 10 vol.% fractionation of biotite, K-feldspar and plagioclase, respectively ($k_{D(mineral/melt}$ from Arth 1976)

bly due to high water activity during melting (e.g. Conrad et al. 1988); therefore, these veins may have been produced at somewhat different melting conditions from sections of the heterogeneous Murzinka protolith.

Granitic Yuzhakovsk veins and Vatikha granites have a similar chemical composition or show common trends. Negative correlation of Sr and Ba with SiO_2, only slightly increasing Rb and relatively constant $K_2O/(CaO+Na_2O)$ point to a combined plagioclase-K-feldspar fractionation (Fig. 10). Similar $^{87}Sr/^{86}Sr_{init}$ and a negative correlation between εNd_{255} and 1/Sr (Fig. 6) also suggest a common genesis from a heterogeneous protolith for HRS granites. Most elements, however, show no definite correlation with εNd_{255}, and the evidence is less unequivocal than in the case of LRS granites. On the basis of the data and field relations we do not consider that the granitic vein plots only coincidentally on the HRS isochron. It appears very unlikely that the apparent decoupling of the Sr and Nd isotopes in HRS and also in LRS granites were caused by post-magmatic homogenisation of the Sr isotopes, due, for instance, to the consistent Rb–Sr whole-rock and single-zircon ages. The correlation of εNd_{255} with several major and trace elements, particularly in the LRS granitoids, is well constrained. This, together with the fairly constant Sm/Nd ratios and Zr and LSEE contents in HRS and LRS granites, does not indicate incomplete Nd isotope equilibration during anatexis or the coincidental distribution of undissolved REE-rich accessories in a melt derived from a homogeneous protolith (cf. Watt and Harley 1993; Ayres and Harris 1997). Since tracer diffusivity of Nd in felsic magmas is one to two orders of magnitude lower than tracer diffusivity of Sr, the initial heterogeneity of the Sr isotopes could have been obliterated, whereas that of Nd isotopes and major elements still exists (Lesher 1994; Perez and Dunn 1996).

Therefore, the large variation of $^{143}Nd/^{144}Nd_{init}$ in the granitoids from Murzinka indicates that their protoliths were highly heterogeneous, having contrasting components with a difference of ~900–1000 Ma in their crustal residence. In the case of the LRS granitoids, the protoliths may be represented by materials derived from young island arcs with minor intercalations of older continental materials. If we also assume a common genesis for the HRS granites, the protolith may be represented by an old metasedimentary sequence injected by younger veins of primitive granitoids, like the situation observed in the neighbouring Osinovsk complex (Fershtater et al. 1994). In both cases the chemical and isotopic variations do not point to simple magma mixing but probably reflect instead the incomplete homogenisation of magmas produced by partial melting of a heterogeneous source region.

Petrogenesis of Dzhabyk granitoids

The major element composition of Dzhabyk granites is comparable to that of granitoids from Murzinka and therefore also to that of partial melts derived from metagreywackes (Fig. 8). Their LREE/HREE, and K/Rb, Rb/Sr and Th/U ratios match that of Murzinka s.s. granites and are compatible with partial melting of felsic material under amphibolite-facies conditions (Bea and Montero 1999). The primitive isotopic composition suggests a protolith rich in juvenile material, although not necessarily the involvement of a parental mantle magma. Instead, the compositional variation and uniform isotope ratios indicate a simple differentiation process. Decreasing Ca, Mg, Fe and Sr contents and Eu anomaly, increasing Rb and $K_2O/(CaO+Na_2O$; Fig. 10) at relatively constant Ba/Sr ratios in Dzhabyk granites are consistent with fractionation of plagioclase in combination with some K-feldspar and an Fe–Mg phase. The low Nd/Th ratios indicate either a protolith rich in thorite or, more likely, fractionation by an Nd-rich and Th-poor mineral, such as amphibole or clinopyroxene (e.g. Bea 1996). If we assume that samples 512 and 509 represent the composition of the initial magma and 588 that of the evolved magma, then the variation in major elements (mass-balance calculation), Rb/Sr and Ba/Sr [Rayleigh law; $k_{D(mineral/melt)}$ from Arth 1976] can be explained by ~45–50% fractionation of a cumulate assemblage consisting of andesine, K-feldspar, quartz, and Mg-hornblende in the proportions of 6:1:2:2 or 4:3:1:1.

Rodnichki and Mochagi granitoids have larger compositional variations, usually with higher Ca, Fe, Mg, K/Rb, Nd/Th and La_N/Yb_N, and a slightly less primitive initial Sr and Nd isotope composition in comparison with Dzhabyk granites. Both rock groups frequently show independent trends (e.g. Figs. 3 and 10), therefore it is regarded as unlikely that Dzhabyk granites derived from the quartz-monzonites by fractional crystallisation. With increasing SiO_2 the $^{87}Sr/^{86}Sr_{init}$, K_2O and Rb increase slightly, whereas the Sr/Rb and Ba/Rb are always higher than in Dzhabyk granites; thus, a different cumulate assemblage was involved in the differentiation of the quartz-monzonitic magma, where weak contamination also took place. The prevalence of rocks with intermediate SiO_2~67% leads us to assume that they represent the initial melt composition. If we use the composition of major rock-forming minerals, sample 808 as starting material and 864 as evolved melt, then the major element (mass-balance calculation) and Rb, Sr and Ba [$k_{D(mineral/melt)}$ from Arth et al. 1976] variations can be modelled with ~48% fractionation of a cumulate (D_{Rb}~0.95, D_{Sr}~2.1 and D_{Ba}~1.9) consisting of andesine (46%), K-feldspar (15.8%), Mg-hornblende (16.2%), biotite (15%) and quartz (7%). The SiO_2-poor varieties likely contain high cumulate proportions. The average composition of 802 and 800, for instance, thereby corresponds approximately to a mixture of 55% initial melt (808) and 45% of the calculated cumulate.

The differences in element abundances and ratios with respect to Dzhabyk granites may be attributed either to differences in the nature and age of the protolith, to partial melting at somewhat higher pressure (e.g. Patiño-Douce 1996), or probably to a combination of both factors. At present we have no criteria to discriminate among these possibilities, but as a working hypothesis we suggest that the granites and quartz-monzonites could have been generated by partial melting of different parts of a thick sequence derived entirely from young island-arc materials. The upper, more felsic part of such a sequence would have produced the granites, whereas the lower, more femic, more alkaline and isotopically slightly more evolved part would have produced the quartz-monzonites by partial melting at higher lithostatic pressure.

In the $^{143}Nd/^{144}Nd$ vs $^{147}Sm/^{144}Nd$ diagram (not shown), Dzhabyk granites and quartz-monzonites, despite their limited variations, do not fit into single lines, defining instead elongated arrays whose longest axis is oblique to the 290-Ma reference isochron. The small variation of $^{143}Nd/^{144}Nd_{init}$ in Dzhabyk granites and quartz-monzonites indicates they come from a protolith formed by materials of similar provenance and age, but with distinct chemical and mineralogical composition; thus, it seems that both batholiths contain two different rock series, which are homogeneous with respect to the initial Sr-isotope composition.

Heat source for crustal melting

The most problematic question regarding the origin of the post-collisional granitoids of the eastern Urals is the origin of the energy input that triggered the partial melting. On one hand, geophysical and structural evidence (e.g. Steer et al. 1998; Brown et al. 1998) indicate that late-orogenic extension was very limited, so that no substantial amount of heat could have been conducted from below. Bea et al. (1997) have attributed the lower Permian remelting of older rocks from West Uralian subduction-related batholiths to underplating by mafic magmas, and have invoked the same mechanism for East Uralian granites due to the similar ages; however, there is no direct evidence for such a mechanism either in Murzinka or in Dzhabyk, except, perhaps, the existence of the younger mafic Kozubaeevsk intrusion in the latter case.

The elevated contents of heat-production elements (HPE: U, Th and K) in granites, on the other hand, suggest that the heat production of protoliths contributed significantly to the thermal evolution of the thickened East Uralian crust. Taking into account the current average U, Th and K concentrations in the Murzinka and Dzhabyk granites, and assuming a melt fraction of 0.3–0.5 with bulk partition coefficients of <0.5 for U, Th and K (e.g. Rollinson 1993), we can estimate the average heat production of their protoliths at around 1.6–2.4 μWm^{-3}. The burial of fertile sources with a heat production of ~2 μWm^{-3} to depths >20 km would cause significant heating of the middle and lower crust in 20–40 Ma (e.g. Fyfe 1973; Patiño-Douce et al. 1990; Gerdes et al. 2000). Since the thickening of the Uralian orogen probably started at ~315 Ma and ~290 Ma in the southern and middle Urals, respectively (Puchkov 1997), or ~30 Ma before the formation of the Dzhabyk and Murzinka granitoids, respectively, we therefore propose that radiogenic heat production played an essential role in the generation of the East Uralian continental-type granites.

Summary and conclusion

The upper-Permian Murzinka batholith is composed of two coeval but chemically and isotopically different rock series that form the two main intrusive units of the batholith, Vatikha and Murzinka s.s, characterised by high and low radiogenic $^{87}Sr/^{86}Sr_{init}$. The granite composition of Vatikha is compatible with partial melting in the granulite facies of a protolith consisting mainly of Proterozoic metasediments. Murzinka s.s. granites, in contrast, were probably generated at lower temperatures from a protolith that comprises mostly material derived from upper-Paleozoic island arcs. The marked Nd isotopic heterogeneity indicates heterogeneous protoliths, containing components of isotopically very different material. The upper-Carboniferous

Dzhabyk batholith is also composed of two coeval but isotopically very similar magmas that yielded granites and quartz-monzonites, respectively. We suggest that these rock series formed by partial melting of different parts of a thick sequence entirely derived from young island-arg.

A characteristic feature of the East Uralian crust therefore seems to be the high amount of Paleozoic island-arc material as a major source for late-orogenic crustal melting. This suggests a fast reworking of juvenile crust during the orogenic evolution of the Uralides which finally caused the generation of peraluminous silicic granitoids, which thus frequently have a mantle-like isotope composition.

The fact that in both batholiths the Rb–Sr whole-rock and Pb–Pb zircon ages match each other nearly exactly indicates Sr isotope equilibration during granite generation, with the $^{87}Sr/^{86}Sr_{init}$ most likely representing the average protolith composition. Nd isotopes, however, were not homogenised, so that the εNd_{init} variations in each rock series reflect the source heterogeneity.

The reasons for post-collisional crustal melting in the eastern Urals are not evident, since geophysical and structural data indicate a lack of significant extension, and no clear evidence exists for massive magmatic underplating. Geochemical data suggest that the elevated heat production of the protoliths, perhaps combined with additional heat from unexposed mafic intrusions, may have played a crucial role in the late-orogenic batholith generation. This process is consistent with the northward-decreasing ages of the continental-type batholiths of ~35 Ma as a result of the oblique collision of the Uralian belt.

Acknowledgements This work was carried out as part of the Uralides-Europrobe project. It was supported by Spanish CICYT grant ref. PB96–1266, European TMR grant URO, and Russian grant 98–05–64826. The help of C. Laurin in improving the English is gratefully acknowledged. We thank A. Cocherie and G. Dias for constructive reviews.

References

Arth JG (1976) Behaviour of trace elements during magmatic processes. A summary of theoretical models and their applications. J Res US Geol Surv 4:41–47

Ayres M, Harris N (1997) REE fractionation and Nd-isotope disequilibrium during crustal anatexis: constraints from Himalayan leucogranites. Chem Geol 139:249–269

Barker F (1979) Trondhjemite: definition, environment and hypothesis of origin. In: Barker F (eds) Trondhjemites, dacites, and related rocks. Elsevier, Amsterdam, pp 1–12

Bea F (1996) Residence of REE, Y, Th and U in granites and crustal protoliths: implications for the chemistry of crustal melts. J Petrol 37:521–552

Bea F, Montero P (1999) Behavior of accessory phases and redistribution of Zr, REE, Y, Th, and U during metamorphism and partial melting of metapelites in the lower crust: an example from the Kinzigite Formation of Ivrea-Verbano, NW Italy. Geochim Cosmochim Acta 63:1133–1153

Bea F, Fershtater G, Montero P, Smirnov V, Zinkova E (1997) Generation and evolution of subduction-related batholiths from the central Urals: constraints on the P–T history of the Uralian orogen. Tectonophysics 276:103–116

Bea F, Montero P, Molina JF (1999) Mafic precursors, peraluminous granitoids and late lamprophyres in the Avila batholith. A model for the generation of Variscan batholiths in Iberia. J Geol 107:399–419

Brown D, Juhlin C, Alvarez-Marron J, Prez-Estaun A, Oslianski A (1998) Crustal-scale structure and evolution of an arc-continent collision zone in the southern Urals, Russia. Tectonics 17:158–171

Conrad WK, Nicholls IA, Wall VJ (1988) Water-saturated and -undersaturated melting of metaluminous and peraluminous crustal compositions at 10 kb: evidence for the origin of silicic magmas in the Taupo Volcanic Zone, New Zealand, and other occurrences. J Petrol 29:765–803

DePaolo DJ (1981) Trace element and isotopic effects of combined wallrock assimilation and fractional crystallization. Earth Planet Sci Lett 53:189–202

Fershtater GB, Borodina NS, Rapoport MS, Osipova TA, Smirnov BH, Levin MY (1994) Orogenic granitoid magmatism of the Urals. Russian Academy of Sciences, Urals Branch, Miacc, 247 pp (in Russian)

Fershtater GB, Montero P, Borodina NS, Pushkarev EV, Smirnov VN, Bea F (1997) Uralian magmatism: an overview. Tectonophysics 276:87–102

Fershtater GB, Bea F, Borodina NS, Montero P (1998) Lateral zonation, evolution, and geodynamic interpretation of magmatism of the Urals: new petrological and geochemical data. Petrology 6:409–433

Fersman AE (1940) Granite pegmatites. Izdateĺstvo AN SSSR, Moskva-Leningrad, 712 pp (in Russian)

Finger F, Roberts MP, Haunschmid B, Schermaier A, Steyrer HP (1997) Variscan granitoids of central Europe: their typology, potential sources and tectonothermal relations. Mineral Petrol 61:67–96

Friberg M, Larionov A, Petrov GA, Gee DG (2000) Paleozoic amphibolite–granulite facies magmatic complexes in the hinterland of the Uralian orogen. Int J Earth Sci 89:21–39

Fyfe WS (1973) The generation of batholiths. Tectonophysics 17:273–283

Gerdes A (1997) Geochemische und thermische Modelle zur Frage der spätorogenen Granitgenese am Beispiel des Südböhmischen Batholiths: Basaltisches Underplating oder Krustenstapelung. PhD thesis, Univ Göttingen, 113 pp

Gerdes A, Wörner G, Finger F (1998) Late-orogenic magmatism in South Bohemia: geochemical and isotopic constraints on possible sources and magma evolution. Acta Univ Carol Geol 42:41–45

Gerdes A, Wörner G, Henk A (2000) Post-collisional granite generation and HT–LP metamorphism by radiogenic heating: the example from the Variscan South Bohemian Batholith. J Geol Soc Lond 157:577–587

Govindaraju K, Potts PJ, Webb PC, Watson JS (1994) 1994 report on Whin Sill dolerite WS-E from England and Pitscurrie microgabbro PM-S from Scotland: assessment by one hundred and four international laboratories. Geostand Newsl 18:211–300

Hamilton W (1970) The Uralides and the motion of the Russian and Siberian platforms. Geol Soc Am Bull 81:2553–2576

Hanson GN (1978) The application of the trace elements to the petrogenesis of igneous rocks of granitic compositions. Earth Planet Sci Lett 38:26–43

Lesher CE (1994) Kinetics of Sr and Nd exchange in silicate liquids: theory, experiments, and applications to uphill diffusion, isotopic equilibration, and irreversible mixing of magmas. J Geophys Res 99:9585–9604

Liew TC, Hofmann AW (1988) Precambrian crustal components, plutonic associations, plate environment of the Hercynian Fold Belt of the central Europe: indications from a Nd and Sr isotopic study. Contrib Mineral Petrol 98:129–138

Montel JM, Vielzeuf D (1997) Partial melting of metagreywackes. 2. Compositions of minerals and melts. Contrib Mineral Petrol 128:176–196

Montero P, Bea F (1998) Accurate determination of $^{87}Rb/^{86}Sr$ and $^{147}Sm/^{144}Nd$ ratios by inductively-coupled-plasma mass spectrometry in isotope geoscience: an alternative to isotope dilution analysis. Anal Chem Acta 358:227–233

Montero P, Bea F, Gerdes A, Fershtater G, Zin'kova N, Borodina N, Osipova T, Smirnov V (2000) Single-zircon evaporation ages and Rb–Sr dating of four major Variscan batholiths of the Urals. A perspective on the timing of deformation and granite generation. Tectonophysics 317:93–108

Patiño-Douce AE (1996) Effects of pressure and H2O content on the compositions of primary crustal melts. Trans R Soc Edinburgh 87:11–21

Patiño-Douce AE, Humphreys D, Johnston AD (1990) Anatexis and metamorphism in tectonically thickened continental crust exemplified by the Sevier hinterland, western North America. Earth Planet Sci Lett 97:290–315

Perez WA, Dunn T (1996) Diffusivity of strontium, neodynium, and lead in natural rhyolite melt at 1.0 GPa. Geochim Cosmochim Acta 60:1387–1397

Pin C, Duthou JL (1990) Sources of Hercynian granitoids from the French Massif Central: inferences from Nd isotopes and consequences for crustal evolution. Chem Geol 83:281–296

Puchkov VN (1997) Structure and geodynamics of the Uralian orogen. Geol Soc Spec Publ 121:201–236

Rollinson HR (1993) Using geochemical data: evaluation, presentation, interpretation. Longman, Harlow

Steer DN, Knapp JH, Brown LD, Echtler HP, Brown DL, Berzin R (1998) Deep structure of the continental lithosphere in an unextended orogen: an explosive-source seismic reflection profile in the Urals (Urals Seismic Experiment and Integrated Studies (URSEIS 1995)). Tectonics 17:143–157

Taylor SR, McLennan SM (1985) The continental crust: its composition and evolution. Blackwell, Oxford

Titterington DM, Halliday AN (1979) On the fitting of parallel isochrons and the method of maximum likelihood. Chem Geol 26:183–195

Vielzeuf D, Holloway JR (1988) Experimental determination of fluid-absent melting relations in the pelitic relations in the pelitic system. Contrib Mineral Petrol 98:257–276

Watt GR, Harley SL (1993) Accessory phase controls on the geochemistry of crustal melts and restites produced during water-undersaturated partial melting. Contrib Mineral Petrol 114:550–566

Wendt I (1986) Radiometrische Methoden in der Geochronologie. Clausthaler Tekt Hefte 23:1–170

York D (1969) Least-square fitting of a straight line with correlated errors. Earth Planet Sci Lett 5:320–324

Zonenshain LP, Kuzmin MI, Natapov LM (1990) Geology of the USSR: a plate-tectonics synthesis. In: Page BM (eds) Geology of the USSR: a plate-tectonics synthesis. Am Geophys Union Geodyn Series 21:27–54